THE EFFECT OF CHROMIUM AND MANGANESE ON THE MECHANICAL PROPERTIES AND CORROSION RESISTANCE OF Al-Si-Fe ALLOY IN 0.5M HCl SOLUTION

BY

ABDULWAHAB, MALIK

DEPARTMENT OF METALLURGICAL ENGINEERING
AHMADU BELLO UNIVERSITY, ZARIA
NIGERIA

AUGUST, 2007

THE EFFECT OF CHROMIUM AND MANGANESE ON THE MECHANICAL PROPERTIES AND CORROSION RESISTANCE OF Al-Si-Fe ALLOY IN 0.5M HCl SOLUTION

BY

ABDULWAHAB, MALIK , B.ENG.(ABU 2002), MNSE, MMSN, MNMS
MSc./ENG./40857/2004-2005

A THESIS SUBMITTED TO THE POSTGRADUATE SCHOOL IN PARTIAL FULFILLMENT OF THE REQUIREMENTS FOR THE AWARD OF MASTER OF SCIENCE IN METALLURGICAL ENGINEERING

DEPARTMENT OF METALLURGICAL ENGINEERING
FACULTY OF ENGINEERING
AHMADU BELLO UNIVERSITY
ZARIA NIGERIA

AUGUST, 2007

DECLARATION

I declare that the work in thesis entitled 'The effect of chromium and manganese on the mechanical properties and corrosion resistance of Al-Si-Fe alloy in 0.5M HCl solution' has been performed by me in the department of metallurgical engineering under the supervision of Dr. I.A. Madugu and Professor O.B. Oloche.

The information derived from the literature has been duly acknowledged in the text and a list of references provided. No part of this thesis was previously presented for another degree or diploma at any university.

Abdulwahab, Malik August, 2007

_____	_____	_____
Name of Student	Signature	Date

CERTIFICATION

This thesis entitled "THE EFFECT OF CHROMIUM AND MANGANESE ON THE MECHANICAL PROPERTIES AND CORROSION RESISTANCE OF Al-Si-Fe ALLOY IN 0.5M HCl SOLUTION" by Abdulwahab, Malik meets the regulation governing the award of the degree of Master of Science of Ahmadu Bello University, Zaria, and is approved for its contribution to knowledge and literary presentation.

_____ Date _____
Dr. I.A. Madugu
Chairman, Supervisory Committee

_____ Date _____
Prof. O.B. Oloche
Member, Supervisory Committee

_____ Date _____
Engr. Dr. S.B. Hassan
Head of Department

_____ Date _____
Prof. S.A. Nkom
Dean, Postgraduate School

DEDICATION

This thesis is dedicated to almighty Allah the most high and the entire member of my family.

ACKNOWLEDGEMENT

All praises and blessings belong to the name of my Lord, may His infinite mercy continue to be showered upon the cream of perfection, the purpose of creation and the reason for continuity Maulana Mustapha Muhammed (SAW), his household and we the belovers till doom day (Ameen).

My appreciation and thanks goes to my supervisors Dr. I.A. Madugu and Prof. O.B. Oloche for their useful corrections, guidance and advice in all the stages of this thesis, it has been of great benefit and experience working with them. May almighty God bless and reward them in all their undertakings (Ameen). Also my profound gratitude to Dr. S.A. Yaro and Mr. V.S. Aigbodion both of Metallurgical Engineering Dept. ABU – Zaria for their assistance during the course of the research. May God reward them accordingly (Ameen).

I sincerely appreciate the encouragement and support of my parents Mal. Abdulwahab O. BELLO and Hajiya Hafusat Abdulwahab and my beloved wife Bilkisu Usman A. and son Yusuf Abdulmalik for their patience and understanding during the research period. I also want to acknowledge my course mate Maigida, H., Bello, K.A. and Balogun S.A. and all members of staff of Metallurgical Engineering Department ABU Zaria for their companionship. May God abundantly bless you all (Ameen).

ABSTRACT

The effect of chromium and manganese on the mechanical properties and corrosion resistance of Al-Si-Fe alloy was investigated. Alloys of varying percentages of Chromium and Manganese from 0.1 to 0.5% (0.1, 0.2, 0.3, 0.4, and 0.5%) with the percentages of iron and silicon kept constant were sand cast into cylindrical test bars of dimension 20mm by 300mm. The mechanical properties (Tensile strength, Hardness and impact energy) of the as-cast and age-hardened alloy samples were determined. Also the corrosion characteristics of the two categories of alloys (as-cast and age-hardened) in 0.5M HCl solutions at room temperature (28^0C) over period of 480hrs were investigated by weight loss method. The results obtained showed an increase in the tensile properties and hardness for the two different alloys with increased Cr and Mn addition. However, the age-hardened samples have improved tensile strength, ductility, hardness, impact energy and corrosion resistance than the as-cast. For example, the highest tensile strength value obtained in the as-cast and age-hardened conditions for Cr is 79.90N/mm^2 and 100.44N/mm^2, Mn is 77.34 N/mm^2 and 98.18 N/mm^2, and MnCr is 82.81 N/mm^2 and 103.23 N/mm^2 respectively. Lowest corrosion rate in the as-cast and age-hardened conditions was at 0.5% (Cr, Mn, MnCr) additions. However, it was also observed that the corrosion rate decrease with increase in the number of days of exposure time for all the alloys. These could be attributed to the corrosion products, formed which tends to shield up corroding surface resulting to a decrease in corrosion rate of the samples investigated.

TABLE OF CONTENTS

TITLE		PAGE
Declaration	- - - - - - - -	ii
Certification	- - - - - - - - -	iii
Dedication	- - - - - - - - -	iv
Acknowledgement	- - - - - - - -	v
Abstract	- - - - - - - -	vi
Table of Contents	- - - - - - - -	vii
List of Tables	- - - - - - - -	x
List of Figures	- - - - - - - -	xii
List of Plates	- - - - - - - -	xiii
CHAPTER ONE		
1.0 Introduction	- - - - - - -	1
1.1 Aims and Objectives	- - - - - -	3
1.2 Background Information / Justification of the Research	-	4
1.3 Scope of the Study	- - - - - -	5
1.4 Statement of the Problem/Limitations of the Study	- -	5
1.5 Contribution to Knowledge	- - - - -	6
CHAPTER TWO		
2.0 Literature Review	- - - - - - -	7
2.1 Al – Si – Fe alloy	- - - - - - -	7
2.2 Ternary and multi-component alloys	- - - -	8
2.2.1 Alloy modification	- - - - - - -	11

2.3 Properties of Aluminium and its alloys - - - - 11

2.3.1 Physical Properties - - - - - - - 11

2.3.2 Mechanical properties - - - - - - 11

2.3.3 Corrosion Properties - - - - - - 12

2.4 Heat treatment of aluminium and its alloys - - - 14

2.4.1 Precipitation Hardening - - - - - - 16

2. 5 Application of aluminium and its alloys - - - - 19

CHAPTER THREE

3.0 Materials and Methods - - - - - - 20

3.1 Materials - - - - - - - - 20

3.2 Equipments - - - - - - - 20

3.3 Methods - - - - - - - - 20

3.3.1 Heat treatment - - - - - - - 21

3.3.2 Corrosion test - - - - - - - 21

3.3.2.1 Corrosion rate determination - - - - - 22

3.4 Microstructural Examination - - - - - 22

CHAPTER FOUR

4.0 Results and Discussion - - - - - - 24

4.1 Results - - - - - - - - 24

4.2 Discussion - - - - - - - - 24

4.2.1 Tensile Strength hardness for as-cast and age-hardened

Al-Si-Fe alloy with Cr, Mn, and MnCr additions - - - 24

4.2.2 Impact energy of the as-cast and age-hardened

Al-Si-Fe alloy with Cr, Mn, and MnCr additions - - - 26

4.2.3 Corrosion Resistance of the as-cast and age-hardened Al-Si-Fe alloy with Cr, Mn, and MnCr additions over the exposure time 26

4.2.4 Microstructural Interpretation of tensile strength and hardness for the as-cast and age-hardened Al-Si-Fe alloy with Cr, Mn, and MnCr additions through grain boundary phenomenon - 27

CHAPTER FIVE

5.0 Summary - - - - - - - - 42

5.1 Conclusion - - - - - - - - 42

5.2 Recommendations - - - - - - - 43

References - - - - - - - 45

Appendix A; micrographs (Plates) - - - - - 50

Appendix B; Graphs (Figures) - - - - - - 58

LIST OF TABLES

TABLES		PAGE
Table 3.1:	Chemical Composition of the produced Alloys - -	23
Table 4.1:	Result of variation of Tensile Properties with % Addition of Chromium for the as-cast alloys - -	31
Table 4.2:	Result of variation Of Tensile Properties with % addition Of Chromium for the age-hardened alloys -	31
Table 4.3:	Result of variation of the Tensile Properties with % addition Manganese for the as-cast alloys -	32
Table 4.4:	Result of variation of the Tensile Properties With % addition Manganese for the age-hardened alloys -	32
Table 4.5:	Result of variation of the Tensile Properties with % addition Manganese-Chromium (MnCr) for the as-cast alloys - - - - -	33
Table 4.6:	Result of Tensile Properties with % Addition Manganese-Chromium (MnCr) For the Aged-Hardened Condition -	33
Table 4.7:	Variation of hardness with % chromium addition for the as-cast alloys - - - - - -	34
Table 4.8:	Variation of hardness with Cr addition for the Age-hardened alloy - - - - - -	34
Table 4.9:	Variation of the Hardness with % manganese addition for the as-cast alloys - - - - -	35
Table 4.10:	Variation of the hardness with % manganese addition for the age-hardened alloys - - - -	35
Table 4.11:	Variation of Hardness with % Manganese – Chromium (MnCr) addition for the as-cast alloys - - -	36
Table 4.12:	Variation of Hardness with % Manganese-Chromium (MnCr) addition for the age-hardened alloys - -	36
Table 4.13:	Variation of the Impact Energies for % Chromium Addition for both as – cast and age – hardened alloys - -	37

Table 4.14: Variation of the Impact Energies for % Manganese Addition for the as – cast and age – hardened alloys - - 37

Table 4.15: Variation of the Impact Energies for %Manganese-Chromium (MnCr) addition for the as–cast and age–hardened alloys 38

Table 4.16: Corrosion Rate of as-cast Al-Si-Fe-Cr alloys in 0.5M HCl Over exposure time (hours) - - - 38

Table 4.17: Corrosion Rate of aged-hardened Al-Si-Fe-Cr alloys in 0.5M HCl Over the exposure time (hours) - - 39

Table 4.18: Corrosion rate of as-cast Al-Si-Fe-Mn alloys in 0.5M HCl Over the exposure time (hours) - - - 39

Table 4.19: Corrosion Rate of aged-hardened Al-Si-Fe-Mn alloys in 0.5M HCl over the exposure time (hours) - - 40

Table 4.20: Corrosion Rate of as-cast Al-Si-Fe-MnCr alloys in 0.5M HCl Over the exposure time (hours) - - 40

Table 4.21: Corrosion Rate of aged-hardened Al-Si-Fe-MnCr alloys in 0.5M HCl Over the exposure time (hours) - - 41

LIST OF FIGURES

FIGURES **PAGES**

Fig. 2.1: Representation of ternary composition - - - 9

Fig. 2.2: Scale for ploting composition on Ternary equilibrium diagram 10

Fig 2.3; Generalized heat treatment cycle for precipitation

hardeneable alloy - - - - - - 17

Fig 2.4: Typical heat-treating cycles for aluminium alloys - - 19

LIST OF PLATES

APPENDIX A (PLATES) **PAGE**

Plate 1: Microstructure of As-cast Al- Si-Fe Alloy - - - - 50

Plate 2: Microstructure of As-cast Al- Si-Fe- 0.1% Cr Alloy- - - 50

Plate 3: Microstructure of As-cast Al- Si-Fe- 0.2% Cr Alloy- - - 50

Plate 4: Microstructure of As-cast Al- Si-Fe- 0.3% Cr Alloy- - - 50

Plate 5: Microstructure of As-cast Al- Si-Fe- 0.4% Cr Alloy- - - 51

Plate 6: Microstructure of As-cast Al- Si-Fe- 0.5% Cr Alloy- - - 51

Plate 7: Microstructure of As-cast Al- Si-Fe- 0.1% Mn Alloy - - 51

Plate 8: Microstructure of As-cast Al- Si-Fe- 0.2% Mn Alloy - - 51

Plate 9: Microstructure of As-cast Al- Si-Fe- 0.3% Mn Alloy - - 52

Plate10: Microstructure of As-cast Al- Si-Fe- 0.4% Mn Alloy - - 52

Plate 11:Microstructure of As-cast Al-Si-Fe-0.5%Mn Alloy- - - 52

Plate 12:Microstructure of As-cast Al-Si-Fe-0.1%Mn-0.1%Cr Alloy - 52

Plate13: Microstructure of As-cast Al- Si-Fe- 0.2% Mn- 0.2%Cr Alloy - 53

Plate14: Microstructure of As-cast Al- Si-Fe- 0.3% Mn- 0.3%Cr Alloy - 53

Plate15: Microstructure of As-cast Al- Si-Fe- 0.4% Mn- 0.4%Cr Alloy - 53

Plate16: Microstructure of As-cast Al- Si-Fe- 0.5% Mn- 0.5%Cr Alloy - 53

Plate17: Microstructure of Age-Hardened Al- Si-Fe Alloy - - - 54

Plate18: Microstructure of Age-Hardened Al- Si-Fe- 0.1% Cr Alloy - 54

Plate19: Microstructure of Age-Hardened Al- Si-Fe- 0.2% Cr Alloy - 54

Plate20: Microstructure of Age-Hardened Al- Si-Fe- 0.3% Cr Alloy - 54

Plate21: Microstructure of Age-Hardened Al- Si-Fe- 0.4% Cr Alloy - 55

Plate22: Microstructure of Age-Hardened Al- Si-Fe- 0.5% Cr Alloy - 55

Plate23: Microstructure of Age-Hardened Al- Si-Fe- 0.1% Mn Alloy - 55

Plate24: Microstructure of Age-Hardened Al- Si-Fe- 0.2% Mn Alloy - 55

Plate25: Microstructure of Age-Hardened Al- Si-Fe- 0.3% Mn Alloy - 56

Plate26: Microstructure of Age-Hardened Al- Si-Fe- 0.4% Mn Alloy - 56

Plate27: Microstructure of Age-Hardened Al- Si-Fe- 0.5% Mn Alloy - 56

Plate28: Microstructure of Age-Hardened Al- Si-Fe- 0.1% Mn-0.1% Cr Alloy - - - - - - - 56

Plate29: Microstructure of Age-Hardened Al- Si-Fe- 0.2% Mn-0.2% Cr Alloy - - - - - - - - 57

Plate30: Microstructure of Age-Hardened Al- Si-Fe- 0.3% Mn-0.3% Cr Alloy - - - - - - - - 57

Plate31: Microstructure of Age-Hardened Al- Si-Fe- 0.4% Mn-0.4% Cr Alloy - - - - - - - - 57

Plate32: Microstructure of Age-Hardened Al- Si-Fe- 0.5% Mn-0.5% Cr Alloy - - - - - - - - 57

APPENDIX B; GRAPHS (FIGURES)

GRAPHS PAGE

Fig. 1: Variation Ultimate Tensile Strength (UTS) with % additions (Cr, Mn, MnCr) for As-cast conditions - - 58

Fig. 2: Variation Ultimate Tensile Strength (UTS) with % additions (Cr, Mn, MnCr) for Age-hardened conditions - 58

Fig. 3: Variation of hardness value with % additions for As-cast conditions - - - - - - - 59

Fig. 4: Variation of hardness value with % additions (Cr, Mn, MnCr) for Age-hardened conditions - - - - - - 59

Fig. 5: Variation of impact energy with % additions (Cr, Mn, MnCr) for As-cast conditions - - - - - - - 60

Fig. 6: Variation of impact energy with % additions (Cr, Mn, MnCr) for Age-hardened conditions - - - - - - 60

Fig. 7: Plot of UTS Vs % Cr additions for both As-cast and Age-hardened conditions - - - - - - 61

Fig.8: Plot of UTS Vs % Mn additions for both As-cast and Age-hardened conditions - - - - - - 61

Fig. 9: Plot of UTS Vs % MnCr additions for both As-cast and Age-hardened conditions - - - - - - 62

Fig.10: Plot of Hardness value Vs % Cr additions for both As-cast and Age-hardened conditions - - - - - - 62

Fig. 11: Plot of Hardness value Vs % Mn additions for both As-cast and Age-hardened conditions - - - - - - 63

Fig. 12: Plot of Hardness value Vs % MnCr additions for both As-cast and Age-hardened conditions- - - - - - 63

Fig. 13: Plot of Impact energy Vs % Cr additions for both As-cast and Age-hardened conditions - - - - - - 64

Fig. 14: Plot of Impact energy Vs % Mn additions for both As-cast and Age-hardened conditions - - - - - - 64

Fig.15: Plot of Impact energy Vs % MnCr additions for both As-cast and Age-hardened conditions - - - - - - 65

Fig.16: Plot of Corrosion rate Vs % of additions (Cr, Mn, MnCr) in 0.5M HCl solution for As-cast condition after 20 days of exposure time - - - - - - - 65

Fig.17: Corrosion rate Vs % of additions (Cr, Mn, MnCr) in 0.5M HCl solution for Age-hardened condition after 20 days of exposure time - - - - - - - 66

Fig.18: Corrosion rate Vs % of additions (Cr, Mn, MnCr) in 0.5M HCl solution for As-cast & Age-hardened condition for 20 days of exposure time - - - - - 66

Fig.19: Corrosion rate Vs % of Cr additions in 0.5M HCl solution for As-cast & Age-hardened condition for 20 days of exposure time - - - - - - - 67

Fig.20: Corrosion rate Vs % of Mn additions in 0.5M HCl solution for As-cast & Age-hardened condition for 20 days of exposure time - - - - - - - 67

Fig.21: Corrosion rate Vs % of MnCr additions in 0.5M HCl solution for As-cast & Age-hardened condition for 20 days of exposure time - - - - - - - 68

Fig.22: Corrosion rate Vs time of exposure (hrs) for Cr addition In the As-cast condition - - - - - - 68

Fig.23: Corrosion rate Vs time of exposure (hrs) for Cr addition in the Age-hardened condition - - - - - 69

Fig. 24: Corrosion rate Vs time of exposure (hrs) for Mn addition in the As-cast condition - - - - - - 69

Fig. 25: Corrosion rate Vs time of exposure (hrs) for Mn additions in the Age-hardened condition - - - - - 70

Fig.26: Corrosion rate Vs time of exposure (hrs) for MnCr addition in the As-cast condition - - - - - - 70

Fig. 27:Corrosion rate Vs time of exposure (hrs) for MnCr additions in the Age-hardened condition - - - - - 71

CHAPTER ONE

1.0 INTRODUCTION

Aluminium and its alloys are characterized by a relatively low density (2.7g/cm^3 as compared to 7.9g/cm^3 for steel and 8.86g/cm^3 for copper), high electrical and thermal conductivities and resistance to corrosion in some common environments such as atmosphere, water: and salt water (William, 1997, Fontana and Greene, 1987, Micheal and James, 1993). These qualities makes aluminum alloys one of the most used non ferrous alloys used in the production of automotives components, construction materials, containers and packaging, marine, aviation, aerospace and electrical industries (Allen, 1979). The good properties and low cost of aluminium alloys have resulted in such increased use that in 1990 aluminium was the second most widely used metal i.e (Second only to steel)(International Aluminium Institute, 2000, Kenneth, 1999) .

Based on these good mechanical properties, the alloys can be forged, stamped, extruded and sand cast (Rajan et al, 1988). Based on the fact that they can be forged to desired shapes at elevated temperatures the can equally be solution treated and aged hardened to obtain desired microstructures and mechanical properties (Nwajagu, 1994 and Rollason, 1964). However, the mechanical properties especially strength of aluminum and its alloy can be enhanced by cold working and alloying, although both processes tend to diminish resistance to corrosion in some alloys (Micheal and James, 1993). Due to the numerous

applications of aluminium in a variety of corrosive environments, different methods/processes have been investigated with the aim of increasing the corrosion resistance of aluminium alloys (William, 1997).

The mechanical properties of aluminium alloys are improved by heat treatment processes such as age-hardening and solution treatment (Michael and James, 1993). Aluminum–silicon-iron alloy provides good combination of cost, strength, and corrosion resistance, high fluidity and is always free from hot shortness (Metals Hand Book, 1975). The compositional specifications of the alloys rest mainly on the amount of iron, silicon, chromium, manganese added as alloying elements in various compositions. Chromium is generally noted for its improvement on strength and resistance to corrosion (Metal Hand Book, 1979A). Manganese is believed to increase toughness, hardenability and counteraction of embrittlement and hot shortness. While iron increases the strength, hardness and reduce tendency to hot cracking and silicon improves the fluidity as well as the castability and some mechanical properties of the cast alloys (Datsko, 1966).

Because of the combined excellent mechanical properties and corrosion resistance, aluminium alloys have found wide applications in aviation, automotive, marine Industries, etc. (Avner, 1974). Although the effects of copper addition on the corrosion behavior of as-cast Al-Si-Fe alloy in acidic media, have been studied by Yaro and Aigbodion, 2006, the authors observed that the addition of Cu to Al-Si-Fe alloy increases its

susceptibility to corrosion attack in the two acidic media used (HCl and $HN0_3$) up to 4% Cu addition. The rate of corrosion is higher in HCl than in $HN0_3$ and the rate of corrosion of coupon in HCl decreased with time (Yaro and Aigbodion, 2006). The Researchers also studied the effect of Cu addition on the mechanical properties of Al-Si-Fe and observed that addition of Cu increased the tensile strength and hardness up to 6% Cu addition (Yaro et al, 2006).

1.1 AIMS AND OBJECTIVES

The aim of the research is to investigate the mechanical properties and corrosion resistance of Al-Si-Fe alloy in 0.5M HCl solution in as-cast condition at room temperature and compare the result with those obtained when the alloys were age-hardened.

The specific aims and objectives of this research was to understand,

1. The individual and simultaneous effects of Cr and Mn addition with Al-Si-Fe alloy on the mechanical properties (tensile properties, hardness and impact strength) in the as-cast condition.
2. The individual and simultaneous effects of Cr and Mn with Al-Si-Fe alloy and age-hardening treatment on the mechanical properties of Al-Si-Fe alloy.
3. To determine the individual and simultaneous effects of concentration of Cr, Mn, MnCr and time of exposure on the corrosion resistance of Al-Si-Fe alloys in 0.5M HCl solution at 28^0C for 480 hrs in the as-cast and age-hardened conditions.

4. To study the microstructural changes that occur as a result of Cr and Mn additions to Al-Si-Fe alloy in as-cast and age-hardened condition
5. The correlation between the studied mechanical properties and microstructures of all the alloys produced.

1.2 BACKGROUND INFORMATION / JUSTIFICATION OF THE RESEARCH

The successful development of aluminium castings in parts and components applications requires, that the casting display a combination of high strength and toughness in thin and thick sections. These properties are determine by the strength and integrity of the microstructures. Though years of research, development and experience, the microstructure characteristics required to achieve these properties in casting have been determined and expressed in a variety of ways. Ultimately, the quality of the microstructures of an alloy determines the performances that can be obtained. However, as reported by Odutola (2005), that all engineering materials are chemically reactive. Hence, the corrosion characteristics of as-cast and age-hardened alloys with individual and simultaneous additions of Cr and Mn in 0.5M HCl solution at 28^0C over a period of 480 hrs. Based on the mechanical properties requirement and corrosion resistance of Al-Si-Fe alloy in automobile industry as oil pan, flywheel and rear-axle housing, crank cases, etc. In aerospace industry as tankages for storage of liquid fuels and oxidizers, engines, airframes, propellers, accessories, etc. This research work improved these properties significantly through alloying and age-hardening treatment.

1.3 SCOPE OF THE STUDY

The study involves determination of the mechanical properties (tensile properties, hardness, and impact strength) of Al-Si-Fe alloy with addition of Cr and Mn in as-cast and age-hardened conditions using standard test procedures. The corrosion test was also carried out on the as-cast and age-hardened samples at room temperature (28^0C) using weight loss method over a period of 480 hrs of exposure time.

1.4 STATEMENT OF THE PROBLEM / LIMITATIONS OF STUDY

There are other important mechanical properties of aluminium and its alloys, but since the service condition is a major factor in selection of the mechanical property to be tested for, other properties have to be investigated. Based on this, the tensile strength, hardness and impact properties were investigated. Despite various ways of evaluating corrosion resistance of metal/alloys, the weight loss method of investigating corrosion was used due to its simplicity and method of result computations.

The HCl acid concentration used for the corrosion test was fixed at 0.5M because it is the optimum concentration of most acids (Yawas, 2005). While the use of the acid as an environment for the samples was as a result of the fact that the alloys found area of applications most in automobiles and aerospace industry. Corrosion due to HCl acid in crude/oil represent a significant portion of the refining cost. In this unit, corrosion comes primarily from chlorides. Chloride corrosion is caused by

hydrogen chloride, which is formed from hydrolysis of the chloride salt contained in the crude. The released hydrogen chloride is relatively non-corrosive in the vapor phase. However, below the dew point of water, hydrogen chloride forms an acidic solution and becomes very corrosive to many structural materials (Quraishi, 2000, 2003) in Yawas (2005). However, some aircraft may be operated in an environment containing ions chloride, sulphate and polluting dust (Odutola, 2005). These chlorides combine with hydrogen gas in the atmosphere forming acid rain which subsequently affects the aircraft components over a period of time. Hence, the use of the HCl solution as the corrosion medium.

1.5 CONTRIBUTION TO KNOWLEDGE

So far, to the best of my knowledge, no previous work has been carried out on the individual and simultaneous addition of Cr and Mn with Al-Si-Fe alloy. Therefore, this research has been able to improve significantly and simultaneously the mechanical properties and corrosion resistance of Al-Si-Fe alloy by alloying and age-hardening treatment.

CHAPTER TWO

2.0 LITERATURE REVIEW

2.1 Al – Si – Fe ALLOY

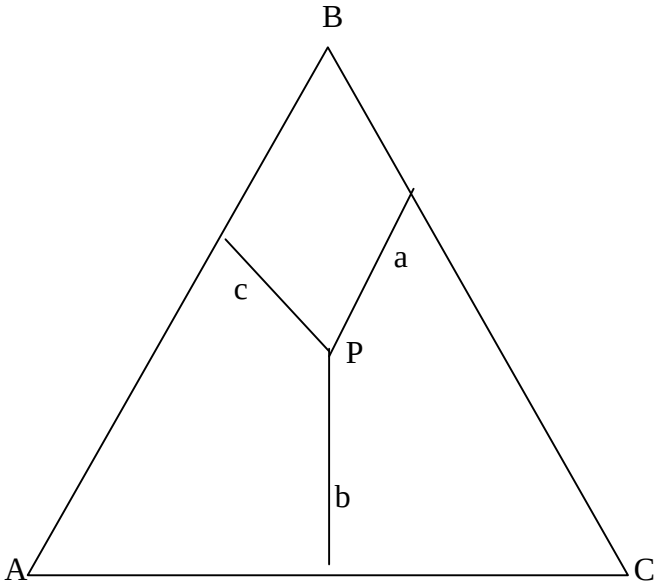
The presence of Si, Mn, Cr and Fe in aluminium causes various precipitates to form during solidification of the alloys (Allen, 1979). The development of dendritic network, precipitation of AlFe phases, eutectic reaction involving the precipitation of Si and Fe phases and formation of complex eutectic phases of $MnAl_2$, $CrAl_2$, $(FeCr)_3$ $SiAl_{12}$, $(FeMn)_3$ $SiAl_{12}$ all took place during the solidification (Rajan et al, 1988). However the formation of these phases depends solely on the composition of the alloys and the cooling rates (Avner, 1974). Manganese and Chromium complexes are easily visible under the optical microscope because of their distinct grayish-white colour tinged with reddish shadings and steel-gray like colour respectively (Brumbough, 1979). While the iron phase is present in both needles (β) and Chinese script form α (Ghosh et al, 2004 and Avner, 1974). The mechanical properties of these alloys are solely dependent and guarded by the composition and the types of phases that are formed and precipitated during the solidification of the alloys immediately after casting (Metal Hand Book, 1979A). Aluminium – Silicon – Iron alloys is also a casting alloy with major alloying element Si followed by iron. The iron content in this alloy in small amount increases the strength and hardness of the alloy and reduces hot - cracking tendencies in casting (Kenneth, 1999). However, it has been known since 1920's that

plates and needles of Al – Si – Fe constituent reduces the strength of aluminium – silicon-casting alloys (Smith, 1981).

2.2 TERNARY AND MULTI COMPONENT ALLOYS

Al-Si-Fe is an alloy with a ternary phase diagram. In particular, any alloy has a unique liquidus temperature for each possible composition of the liquid, and similarly, it has a unique solidus temperature for each compositions of the solid. An important difference from the two - component case is that, in systems of three or more components, the temperature does not uniquely define the solidus and liquidus compositions, in general. The simplest example is that of the ternary system; compositions in ternary systems are usually represented as points on or in an equilateral triangle, ABC (in fig. 2.1). The corners of the triangle correspond to the three pure components, and the edges represent the three binary systems. Each point within the triangle corresponds to a definite composition; the ratio of the three components for the P is equal to the ratio of the distances a,b,c, of P from the three sides of the triangle. The sum of these three distances is constant for a given equilateral triangle (Rhines, 1956). Since each possible composition of liquid corresponds to a point on or in the triangle, it follows that the liquidus is a surface, rather than a line as in the “two-component” case. In a three-component system therefore there must be a line on a liquidus surface that corresponds to any particular temperature, The ties lines are

mostly used to indicate the equilibrium relationships (IAI, 2006 and Chalmers, 1964).



- Pa + Pb + Pc = constant

Fig. 2.1: Representation of ternary composition (Chalmers, 1964)

The composition of a four-component alloy could, in principle, be represented by a point in a tetrahedron, by analogy with the representation of a ternary composition by a point in a triangle; but there is no possible geometrical method for representing quaternary or higher phase diagrams, in which an extra dimension is required to represent temperature (Chalmers, 1964). According to Pascoe, for plotting the equilibrium diagrams of ternary alloys, that is, alloys made of three components; three independent variables have to be considered. Two are necessary to specify the composition, and the third is temperature. A three-dimensional space model is therefore necessary to show the phases present for any composition and temperature (as showed in Fig. 2.1). The

most convenient form of diagram is that with an equilateral triangle as base and a temperature axis perpendicular to this base. The three perpendiculars to the sides of an equilateral triangle from any point P within the triangle have a constant sum whatever the position of P. If this sum be taken as 100% then the three perpendicular distances can be used to represent the proportions of the three components (Figs. 2.1 & 2.2), the distances Pa, Pb, and Pc can represent the proportions of element A,B, and C respectively. The equilateral triangle can be divided up as in (Fig. 2.2) and the composition corresponding to any point can be read directly. The side AB will represent binary alloys of element A & B. the first line parallel to this side will represent an alloys containing 10%C (Pascoe, 1962).

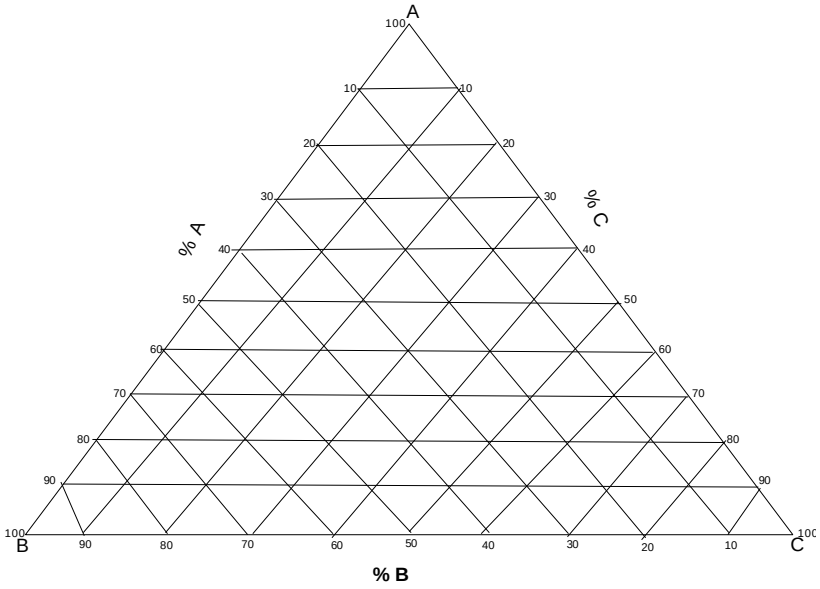


Fig. 2.2: Scale for Plotting Composition on Ternary Equilibrium Diagrams (Pascoe, 1962)

2.2.1 Alloy Modification

In order to meet the mechanical performance of most aluminium alloys, typical modification and heat treatment is done. Alloy modification alters the morphology of the acicular aluminium silicon eutectic into a finer, more interconnected fibrous phase improving toughness and ductility. Both sodium and strontium modification have been used historically during casting (Thompson et al, 2004).

2.3 PROPERTIES OF ALUMINIUM AND ITS ALLOYS

2.3.1 Physical Properties

There is no significant variation in most physical properties from one alloy to another, with the exception of electrical and thermal conductivity. The specific gravity of wrought alloys varies from about 2.65 to 2.80; for cast alloys the range is about 2.50 to 2.95 (2.5 or less for Li – Al Alloys). The modulus of elasticity varies from 10 to 10.4 x 10^6 PSi (70 to 72 GPa) (Rollason, 1964)

Coefficient of expansions for wrought alloys vary from about 12.4 to 13.3; for cast alloys the range is about 10.5 to 14.0. Aluminium alloys have higher conductivities (electrical and thermal) than most metals, and they are cheaper than the alloys that are better conductors (copper, silver, gold, and so on) (Kenneth, 1999).

2.3.2 Mechanical properties

In the 1970's and 1980's a considerable number of researches were carried out with the aim of improving the mechanical properties of

aluminium alloys. The most significant among them are Li – Al alloys and Metal Matrix Composites (MMC) with aluminium as the matrix (Kenneth, 1999).

The hardness of aluminium alloys vary from about 20HB to about 120 HB, but this usually has no significance in selection for mechanical properties as the hardest aluminium alloy is softer than most soft steel. For aluminium alloys, hardness is not an indication of wear resistance but an indicator of machinability because an alloy of high hardness is likely to have better machinability than an alloy of low hardness. The tensile properties of aluminium alloys vary from 90MPa for pure aluminium to as high as 676MPa for a zinc-copper-magnesium alloy in the age-hardened condition (Kenneth, 1999).

The strength of aluminium cast alloys depends on the casting technique as the metal mould processes with fast cooling rates usually give higher strength than sand-cast alloys. Casting alloy systems include alloys of aluminium and Si, Cu–Si, Mg, and Si –Mg, Zn –Mg, and Si – Ni, Mg – Cu (Kenneth, 1999).

2.3.3 Corrosion Properties of aluminium and its alloys

Aluminium and it alloys are considered to be highly corrosion resistant under the majority of service conditions (Fontana and Greene, 1987). The various grades of pure aluminium are most resistant, followed closely by the Al – Mg, Al – Mn alloys. Next in order is Al – Mg – Si and then Al – Si alloy. The alloy containing copper are the least resistant to corrosion; but

this can be improved by coating each side of the copper containing alloy with a thin layer of high purity aluminium, thus gaining a three – ply metal, i.e. Alclad. This cladding acts as a mechanical shield and also protects by sacrificial; corrosion at cut edges (Rollason, 1964). When aluminium surface are exposed to the atmosphere, a thin, invisible oxide (Al_2O_3) skin forms, which protects the metal from corrosion in many environments. This oxide film forms in many environments, but it can be artificially produced by passage of electric current. This process is called anodizing (Fontana and Greene, 1987). This film protect the metal from further oxidation, unless this coating is destroyed, the material remains fully protected against corrosion (Avner, 1974).

The types of corrosion that affect Al-alloys are galvanic, stress corrosion cracking, inter-granular, Crevice (Fontana and Greene, 1987; Michael and James, 1983; Greenfield, 1971; Metal Hand Book, 1966; Barer and Peters, 1974; Carter, 1977).

Studies carried out on the corrosion behaviour of aluminium based alloys in caustic soda of varying concentration Al-1.2%Mn – 1.0%Mg, Al – 0.6%Mn – 1.5%Mg – 4.4%Cu and 98.9%Al showed that in all the concentration, the corrosion rate profile has an initial steep rise followed by subsequent fall for all the alloys but with progressive severity of attacks following the order: 98.9%Al, Al – 1.2%Mn – 1.0%Mg and Al – 0.6%Mn – 1.5%Mg – 4.4% Cu (Idenyi and Neife, 2005)

2.4 HEAT TREATMENT OF ALUMINIUM AND ITS ALLOYS

Aluminium and its alloy are classified into two main groups; heat treatable and non-treatable. The aim of heat treatment is to change the microstructure and mechanical properties of metals and alloys. In aluminum alloys, the basic aim of heat treatment is to increase strength and hardness depending on the rate of heating and cooling. The properties can be varied according to requirement (Rajan et al, 1988). The main types of heat treatments employed with aluminium and its alloys include annealing, stress-relieving, solution treatment and precipitation hardening, otherwise known as age-hardening (Allen, 1979).

Heat treatment processes for increasing the strength and hardness of either wrought or cast aluminium alloys utilize the mechanism of precipitation hardening. One essential attribute of a precipitation hardening alloy system is the temperature and time dependent equilibrium solid-solubility. This is characterized by decreasing solubility with decreasing temperature and then followed by solid-state precipitation of second phase atoms on cooling in the solidus region. These conditions are usually met by most aluminium equilibrium systems of heat-treatable types, such as the Al-Si and Al-Cu alloys etc (Metal Hand Book, 1981). The first stage of precipitation can be made to occur at room temperature and this is called natural ageing while subsequent precipitations can be accelerated by heating the alloy to slightly above the room temperature and then cooling in air, which is referred to as artificial ageing.

Precipitation heat-treatment for the purpose of increasing strength and hardness is a three-step process.

The first step is the solution heat-treatment that involves dissolution of soluble phases followed by quenching for the development of super-saturation and then ageing which is the precipitation of solute atoms either at room temperature (natural ageing) or elevated temperatures (artificial ageing) (Metal Hand Book, 1981). Solution heat-treatment: In order to take the advantage of the precipitation hardening reaction, it is necessary first to produce a solid solution. Production of a solid solution consists of soaking the aluminium alloy at a temperature sufficiently high and for such a time so as to attain an almost homogeneous solid solution. The soaking time is required to achieve a satisfactory degree of dissolution of the undissolved or precipitated soluble phase constituents and for attainment of a reasonable degree of homogeneity (Markandeya et al, 2004).

Quenching is carried out to avoid slow cooling which may result in the precipitation of phases that may be detrimental to the mechanical properties or to the corrosion resistance of the alloys. For these reasons solid solutions formed during solution heat-treatment are quenched rapidly without interruption to produce a supersaturated solution at room temperature (Metal Hand Book, 1981).

Precipitation heat-treating is used to impart high strength and hardness to aluminium alloys. Generally artificial ageing imparts higher strength and hardness values to aluminium alloys without sacrificing other mechanical

properties and also improves the resistance of these alloys to exfoliation and stress- corrosion cracking (Metal Hand Book, 1979A, Gayle and Vadersande, 2004, Datsko, 1966).

2.4.1 Precipitation Hardening

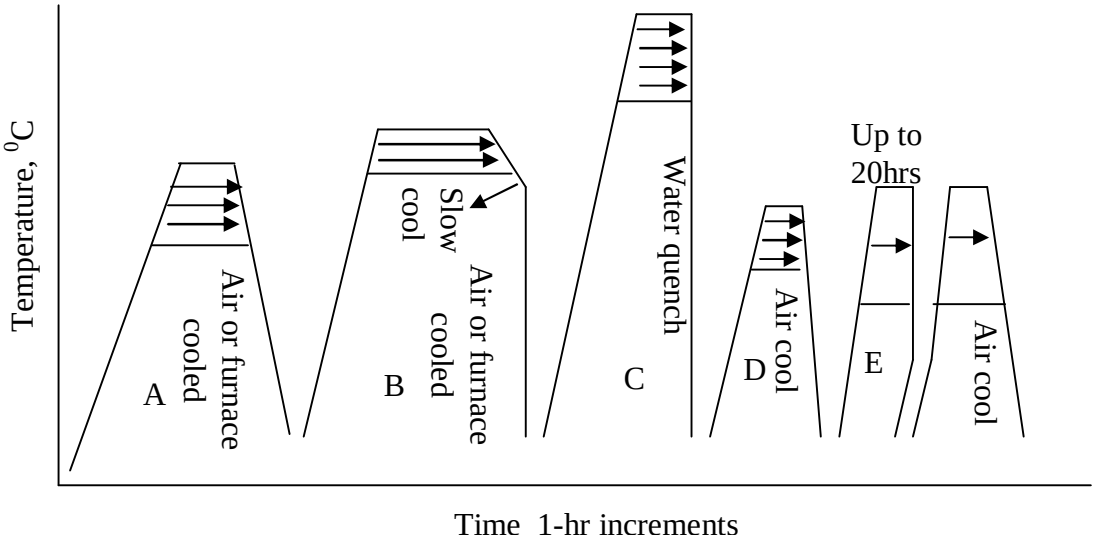
Precipitation hardening or age-hardening or dispersion hardening heat treatment techniques is used to strengthen malleable materials, especially non-ferrous alloys including most structural alloys of aluminium and titanium (www.answers.com/topic/precipitation-hardening, 2007). After quenching, precipitation of second-phase particles occurs. Precipitation with time at room temperature is called natural ageing, whereas precipitation of higher temperatures is referred to as artificial ageing. The hardness after solution treatment is comparatively low. The maximum hardness and strength develops when alloy is aged at a suitable temperature that normally ranges between 120^0C and 200^0C. In some cases the ageing temperature may be as high as 300^0C. Ageing time may vary from 4 to 24hours. Spontaneous decomposition of supersaturated solid solution takes place during ageing treatment. Ageing temperature and degree of super-saturation play a great role on the final properties of the alloy. The higher the ageing temperature and degree of super-saturation the faster the ageing. Ageing is adopted where more stable phase is required together with dimensional stability. This process is also called stabilizing ageing. Besides mechanical properties, physicochemical properties are also affected by ageing. This happens due to metastable

structure of the alloy, which are formed during ageing of supersaturated solid solution obtained by solution treatment. Rise in temperature changes the atomic position with corresponding changes in the forces associated with inter-atomic bonds. At the same time distribution of second-phase particles also changes (Rajan et al, 1988 and www.key-to-metals.com/article7.htm,2007). For example, in Al-Cu alloys, the increase in strength that occurs with the passage of time at room temperature in a solution-heat treated alloy is thought to be caused by the gradual precipitation of the $CuAl_2$ phase in very fine submicroscopic particles. This precipitation takes place at the aluminium grain boundaries and along crystallographic planes within the aluminium crystals. A very fine particle of $CuAl_2$ precipitate act as keys and build up resistance to slip thereby greatly increasing the strength of the alloy (Allen, 1979).



Fig 2.3: Generalized heat treatment cycle for precipitation hardeneable alloy (Allen, 1979)

Figure 2.3 shows a typical heat treatment cycle suitable for a precipitation hardeneable alloy. In this case, the alloy is heat treated and held at high temperature (solutionizing). The alloy is then cooled rapidly at room temperature by quenching. The quenched alloy is heated and held at a moderately high temperature above the room temperature, followed by slow cooling. The last step is termed artificial ageing (Rajan et al, 1988, www.key-to-metals.com/article7.htm,2007 and www.secant.net,2002). It has been reported by Hansen et al, 2004 that when ageing is conducted in the low temperature region, little effect of quenching is seen on mechanical response, and that a continuous change in properties; hardness, strength, electrical conductivity, etc., reflect a gradual change of size, composition and internal order in zones and precipitates, as well as in their abundance (Hansen et al, 2004).



A – Anneal to remove cold work

B – Anneal to soften heat treatment alloys

C – Solution treatment

D – Stress relieve

E – Age hardening (artificial)

Fig 2.4: Typical heat-treating cycles for aluminium alloys (Kenneth, 1999).

2.5 APPLICATION OF ALUMINIUM AND ITS ALLOYS

The properties of aluminium that makes it and its alloys the most economical for a wide variety of uses are appearance, fabricability, physical or mechanical properties, corrosion resistance and a combination of these properties. Some of these areas of applications are; aerospace, automotive, railroad, marine, electrical, construction, application as household utensils, and application as packaging materials (Metal Hand Book, 1979A, 1981 and IAI, 2000).

CHAPTER THREE

3.0 MATERIALS AND METHODS

3.1 Materials

The materials used for this research for the production of Al-Si-Fe (control), Al-Si-Fe-Cr, Al-Si-Fe-Mn and Al-Si-Fe-MnCr alloy systems includes high purity aluminum obtained from Northern Cable Company NOCACO Kaduna and ferroalloys (FeSi, FeCr, FeMn), etchants, baker, hydrochloric acid, thread (for suspending the coupons in media), measuring cylinder, silica sand and bentonite, moulding boxes from National Metallurgical Development Center (NMDC), Jos.

3.2 Equipments

The following equipment were used, Muffle electrical resistance furnace, Denison impact tester, Rockwell Hardness B Scale machine, Tinius Olsen tensile testing machine, Polishing machine, Metallurgical microscope, Digital weighing balance.

3.3 Methods

Sixteen different compositions of alloys were produced in which the amounts of Mn and Cr in the alloys were varied from 0.1 to 0.5% in step of 0.1% while the percentages of Si and Fe were kept constant (Table 3.1). Each composition was melted separately in alumina crucible. The melting was done using a muffle resistance furnace that was allowed to heat to 750^0C before the crucible was removed and other alloying elements (ferroalloys) added. Then the crucible was returned in to the furnace for

further 30 minutes during which the furnace temperature was raised to 800^0C for superheat to occur; then 0.01%NaCl was added and stirred thoroughly before pouring into the mould. The cast samples were machined to standard tensile, hardness, impact, and corrosion test specimens.

3.3.1 Heat Treatment

Some of the machined samples were solution heat treated at temperature of 490^0C in an electric heat treatment furnace, soaked for six hours at this temperature and then rapidly quenched in warm water. The quenched specimens were then aged at 200^0C for six hours before cooling in air.

3.3.2 Corrosion Test

A total of 320 corrosion coupons were used for the research, 160 each for as-cast and heat treated respectively. Before immersion, the coupons were cleansed, weighed and stored in the desiccators. Sets of same concentrations of 0.5M HCl solution were prepared (one for the as-cast and the other for the age-hardened samples). The cleaned coupons were suspended in the HCl solutions with the aid of threads. The weight losses of the coupons were taken at intervals of two days over a period of twenty (20) days. After removal from the solution, each coupon was weighed. The surface was scrubbed with brush in distilled water, rinsed in ethanol and then air-dried.

3.3.2.1 Corrosion Rate Determination

The weight loss method of estimating the corrosion rate was employed. The weight loss was determined by finding the difference between the initial weight of the coupon and the final weight after two (2) days interval using the following relationship,

$W = W_0 - W_f$

The corrosion rate was determined in mils per year (mpy) using relationship (Fontana and Greene, 1987).

$$\text{Corrosion rate (mpy)} = \frac{534W}{DAT} \quad \text{- - - equation (3.1)}$$

Where,

W = Weight loss ((mg), D = Density of the material, g/cm^2;

A = Cross-sectional area, in^2 T = Exposure time, hrs;

W_0 = Initial weight of coupon W_f = final weight of the coupons.

3.4 MICROSTRUCTURAL EXAMINATION

Metallographic specimens were cut from the as-cast and age-hardened alloys. The cut specimens were then mounted in Bakelite and mechanically ground progressively on grades of SiC impregnated emery paper (80-600 grits) sizes using water as the coolant. The ground specimens were then polished using one-micron size alumina polishing powder suspended in distilled water. Final polish was done using 0.5-micron alumina polishing powder suspended in distilled water. Following the polishing operation, etching of the polished specimen was done using Keller's reagent and the structures obtained were then photographically

recorded using an optical microscope with built in camera and are given in Plates 1 to 32.

Table 3.1: Chemical Composition of the produced Alloys

S/N	% Si	%Fe	%Cr	%Mn	%Al
1	2.1	0.7	0	-	97.2
2	2.1	0.7	0.1	-	97.1
3	2.1	0.7	0.2	-	97.0
4	2.1	0.7	0.3	-	96.9
5	2.1	0.7	0.4	-	96.8
6	2.1	0.7	0.5	-	96.7
7	2.1	0.7	-	0.1	97.1
8	2.1	0.7	-	0.2	97.0
9	2.1	0.7	-	0.3	96.9
10	2.1	0.7	-	0.4	96.8
11	2.1	0.7	-	0.5	96.7
12	2.1	0.7	0.1	0.1	97.0
13	2.1	0.7	0.2	0.2	96.8
14	2.1	0.7	0.3	0.3	96.6
15	2.1	0.7	0.4	0.4	96.4
16	2.1	0.7	0.5	0.5	96.2

CHAPTER FOUR

4.0 RESULTS AND DISCUSSION

4.1 Results

The results obtained are presented in tabular (table 4.1-4.21) and graphical form (Appendix B). Tables 4.1-4.21 are given the determined mechanical properties and Corrosion rates of the alloys. Figures 1 –15 show the variation of mechanical properties with percentage Cr and Mn addition while in Figures 16 – 27 are given the variation of corrosion rates with exposure time and percentage Mn and Cr addition for the categories of alloys (as-cast and age-hardened). The microstructures of the as-cast and age-hardened alloys are presented in Appendix A (Plates 1 – 32).

4.2 Discussion

4.2.1 Tensile Strength and Hardness for as-cast and age-hardened Al-Si-Fe alloy with Cr, Mn, and MnCr additions

From the results obtained in this research, it can be seen that the Ultimate Tensile Strength (UTS) and the hardness of the alloys increase with increase in Cr and Mn additions for both the as-cast and age-hardened conditions (Tables 4.1 – 4.12) but dropped sharply at 0.5% for Mn and MnCr additions only (Table 4.9 – 4.12). The reason for this sharp drop in the tensile strength and hardness beyond 0.4% (Mn and MnCr) for the as-cast and age-hardened alloy may be as a result of the excess addition forming softer phases which subsequently reduce the strength and hardness of the alloys (Figures 1- 4 and 7-12). However, age-hardened

alloys have higher UTS and hardness values. The reason for the increase in ultimate tensile strength as the percentage Cr was increased for both the as-cast and Age-hardened alloys may be as a result of the formation of fine grain complex precipitates of $CrAl_2$ and $(Fe)_3$ $SiAl_{12}$ in the matrix and serves as a barrier to movement of dislocations, hence the increasing strength and hardness of the alloys. However, better mechanical properties upon addition of chromium can be explained thus; that chromium has a slow diffusion rate and forms fine dispersed phase (www.key-to-metals.com, 2007). These dispersed phases inhibit nucleation and grain growth; these phases interfere with dislocation, hence higher strength. Also, the explanation for the increase in the ultimate tensile strength and hardness as the percentage manganese increases up to 0.4% and then fell sharply at 0.5% Mn may be probably as a result of the formation of fine dispersoid of (Mn, Fe) Al_6 and α (Al-Si-Fe-Mn) constituents, and the manganese –rich precipitate nucleate preferentially and create a pinning action. These actions inhibited the movement of the dislocations, hence increasing the strength and hardness of the alloys. This also agree with the statement that Mn increases strength either in solid solution or finely precipitated intermetallic phase and has no adverse effect on corrosion resistance. Iron has a high solubility in molten aluminium and is therefore easily dissolved at all molten stages of production and most of iron present in aluminium has an intermetallic second phase in combination with aluminium and often other

elements (www.key-to-metal.com, 2007). This particle of the second phase in the structure pinned down slip, which in turn constitute better strength to the alloys.

4.2.2 Impact Energy of the as-cast and age-hardened Al-Si-Fe alloy with Cr, Mn, and MnCr Additions

From the results, the impact energy decreased for all percentages of Cr and Mn additions for both as-cast and age-hardened samples with the age-hardened having better impact properties than the as-cast (Figures 5-6 and 13-15). This observation tally with the fact that small amount of chromium improves the impact energy of aluminium alloys (Allen, 1979 and www.key-to-metals.com, 2007). This is clearly shown in tables 4.13 – 4.15. For example highest impact energy obtained from the alloys for chromium additions are 39J (Cr; as-cast) and 82J (Cr; age-hardened).

4.2.3 Corrosion Resistance of the as-cast and age-hardened Al-Si-Fe alloy with Cr, Mn, and MnCr additions over the exposure time

In Tables 4.16-4.21 i.e Figures 16-21 it can be seen that, the corrosion rate decreases for both as-cast and age-hardened alloys as the amount of Cr and Mn was increased with the age-hardened possessing better corrosion resistance than the as-cast. The reason for the lower corrosion rate of age-hardened samples may be due to the precipitation of the intermetallic compounds and the amount of the intermetallic precipitated increase with increase in Cr and Mn additions. It could be observed in table 4.20 – 4.21 i.e. Figure 16-17 that simultaneous addition of chromium

and manganese to Al-Si-Fe alloy in the as-cast and age-hardened conditions have better corrosion resistance to the alloy due to the formation of hard and passive phases that acted as strong protective barriers to corrosion. Specifically, Figures 19-22 show that after 480 hrs exposures, 0.5% (Cr, Mn and MnCr) alloys have the best corrosion resistance for both as-cast and age-hardened conditions. Generally, it can be seen in Figures 22 – 27 that for as-cast and the age-hardened conditions, the corrosion rates decrease with increase in exposure time for all levels of additions. The trend agreed with Yaro and Aigbodion, (2006) and Idenyi and Neife, (2005). From Tables 4.16-4.21, corrosion of the alloys was not significantly seen for all levels of Mn and Cr additions up to 8 days (192 hrs) because the protective film formation of the alloys has not been damaged.

4.2.4 Microstructural Interpretation of Tensile Strength and Hardness for the as-cast and age-hardened Al-Si-Fe alloy with Cr, Mn and MnCr additions through grain boundary phenomenon

From the microstructures (plates), grain boundaries on the microstructures can be used to explain the mechanical behavior of the alloys. Plates 2-6 and 18-22 showed an increase in fineness of the interdendritic network and many grain boundaries (but smaller in sizes) are formed. Same observation seen in Plates 7-10, 12-15, 23-26 and 28-31. The reasons for this is that grain boundaries or other factors (solute atom, particles of the second phase in the structure and other dislocations; the concept of work-

hardening) are the factors that interfere or inhibit the movement of dislocation and once the grain boundaries are many, this means more barriers to dislocation motion hence increase in the strength and hardness of the alloys. But the network in Plates 11, 16, 27 and 32 differs; grain sizes within the matrix are coarser. However, more coarse grain sizes result in decrease in strength. This has been shown by various expressions (George, 1981). That is, Hall and Petch emphasized the role of grain boundaries in causing nonhomogenous deformation and introducing multiple slip. They empirically established a relationship between the tensile yield stress and grain size.

$$\sigma_0 = \sigma_i + K' \frac{1}{\sqrt{D^2}}$$ ---------- Equation (4.1)

Where:

σ_0 = yield stress,

σ_i = friction stress opposing motion of dislocation,

K' = "unpinning constant" measuring the extent to which dislocations are piled up at barriers

D = grain diameter

There are two models for explaining this. The first is based on the concept that grain boundaries act as barriers to dislocation motion. This model was the basis for explaining grain boundary relationship with mechanical properties studied in this research work. However, the use of Transmission Electron Microscopy (TEM), that is, to show micrograph of

dislocations piled up at different grain boundaries. The term σ_i depends strongly on temperature, strain and alloy (impurity) content. The second models for the grain-size dependence of flow stress, does not require the presence of dislocation pile-ups at grain boundaries. This model avoids the description of the stresses at grain boundaries and instead concentrate on the influence of grain size on the dislocation density, and hence, on yield or flow stress. The flow stress is given in terms of dislocation density;

$\sigma_0 = \sigma_i + \alpha G b \rho^{1/2}$ ---------- Equation (4.2)

Where

α = numerical constant, generally between 0.3 to 0.6

ρ = dislocation density (inverse of grain diameter). Generally, most grain-size measurements seek to correlate the interaction of grain boundaries with a specific mechanical property (George, 1981).

However, after age-hardening the alloy, the variation in the mechanical properties is in line with past researches that the effects of precipitation on mechanical properties are greatly accelerated by reheating the quenched material to about 100-200^{0}C. The characteristic feature of elevated-temperature ageing effects on tensile properties is that the increase in yield strength is more pronounced than the increase in tensile strength. At higher ageing temperature, the precipitate particles appear more ordered and strengthening by ageing is a result mainly of interactions between dislocations and precipitates by shearing, or Orowan

mechanism with less contribution from the surrounding strains. Also ductility, as measured by percentage elongation, decreases (www.key-to-metals.com, 2007, www.key-to-metals.com/article7.htm, 2007, Hansen et al, 2004).

Plate 1 is the microstructure of the control sample while Plates 2-16 are the microstructures of the as-cast sixteen alloys of different compositions and Plates 17-32 are the microstructures of the age-hardened samples. The control sample in the as-cast condition shows interdendritic structures of silicon eutectic in the matrix of aluminium solid solution. This network structure upon addition of the alloying elements (Cr and Mn) forms precipitates (Plates 2-16) such as $CrAl_6$, $CrAl_2$, $FeAl_3$, $FeAl_6$, Fe_3SiAl_{12} ,$(FeMn)_3SiAl_{12}$,$MnCrAl_6$ particles within the matrix. But after age-hardening the alloys, the microstructures revealed a general breakdown of the network and phases become finer as the addition of the alloying element was increased (Plates 17-32). The details and interpretation (Metal Hand Book, 1979B) of the microstructures are well explained in Appendix A (Plates).

Table 4.1: Result of variation of Tensile Properties with % Addition of Chromium for the as-cast alloys.

%Cr addition	% E	%RCSA	Yield load (N)	Yield strength N/mm^2	Maximum load (N)	UTS N/mm^2
Control	4.0	7.8	3800	31.00	4138	33.72
0.1	4.1	7.8	4091	33.34	6800	55.40
0.2	2.8	5.0	5000	40.75	8000	65.20
0.3	2.2	4.7	6000	48.90	8282.3	67.50
0.4	1.0	3.2	6800	55.40	8399.7	68.46
0.5	1.0	3.2	7899	64.38	9804	79.90

Table 4.2: Result of variation Of Tensile Properties with % addition Of Chromium for the age-hardened alloys

%Cr addition	% E	%RCSA	Yield load (N)	Yield strength N/mm^2	Maximum load	UTS N/mm^2
Control	5.0	10.9	4981.6	40.6	6800	55.40
0.1	6.0	15.3	6900	56.20	8399.7	68.46
0.2	6.0	15.3	7200	58.70	9804	79.90
0.3	5.4	9.3	7800	63.57	9828.3	80.10
0.4	4.4	7.8	9804	79.90	11256	97.40
0.5	4.0	7.8	9804	79.90	12324	100.44

Table 4.3: Result of variation of the Tensile Properties with % addition Manganese for the as-cast alloys.

%Mn addition	% E	%RCSA	Yield load (N)	Yield strength N/mm^2	Maximum load (N)	UTS N/mm^2
Control	4.0	7.8	3800	31.00	4138	33.72
0.1	4.1	7.8	4800	39.12	5269	42.94
0.2	2.2	4.7	4920.3	40.10	7786.5	63.46
0.3	2.0	4.0	5158	42.04	8095	65.95
0.4	1.0	3.2	6800	55.40	9488	77.34
0.5	0.8	2.5	6667.41	54.34	8719	71.06

Table 4.4: Result of variation of the Tensile Properties With % addition Manganese for the age-hardened alloys.

%Mn addition	% E	%RCSA	Yield load (N)	Yield strength N/mm^2	Maximum load	UTS N/mm^2
Control	5.0	10.9	4981.6	40.6	6800	55.10
0.1	5.0	10.9	6800	55.40	7786.5	63.46
0.2	5.0	10.9	7000	57.00	8719	71.06
0.3	4.2	7.8	7400	60.30	8757	76.15
0.4	2.0	4.7	8400	68.46	12044	98.18
0.5	2.0	4.7	7800	63.57	11576.8	94.35

Table 4.5: Result of variation of the Tensile Properties with % addition Manganese-Chromium (MnCr) for the as-cast alloys.

%MnCr addition	% E	%RCSA	Yield load (N)	Yield strength N/mm^2	Maximum load	UTS N/mm^2
Control	4.0	7.8	3800	31.00	4138	33.72
0.1/Mn-0.1Cr	3.0	6.2	4800	39.12	5935	48.37
0.2Mn-0.2Cr	2.2	4.7	5391.5	43.94	6069	49.46
0.3Mn-0.3Cr	2.0	4.0	6667.4	54.34	8806	71.77
0.4Mn-0.4Cr	0.8	2.5	7411.1	57.10	10161	82.81
0.5Mn-0.5Cr	0.4	1.5	7005.2	60.40	9515	77.55

Table 4.6: Result of Tensile Properties with % Addition Manganese-Chromium (MnCr) For the Aged-Hardened Condition.

%MnCr addition	% E	%RCSA	Yield load (N)	Yield strength N/mm^2	Maximum load	UTS N/mm^2
Control	5.0	10.9	4981.6	40.6	6800	55.40
0.1/Mn-0.1Cr	6.0	10.9	7000	57.00	8806	71.77
0.2Mn-0.2Cr	5.0	10.9	7200	58.70	10161	82.81
0.3Mn-0.3Cr	4.0	7.8	8000	65.20	12257	99.89
0.4Mn-0.4Cr	2.0	3.2	10700	87.20	12606	103.23
0.5Mn-0.5Cr	1.4	1.6	9600	78.20	11901.9	97.00

Table 4.7: Variation of hardness with % chromium addition for the as-cast alloys.

%Cr addition	1st HRB	2nd HRB	3rd HRB	Mean HRB
Control	14.0	13.0	14.0	13.7
0.1	20.0	19.0	20.0	19.7
0.2	24.0	22.0	20.0	22.0
0.3	30.0	25.0	26.0	27.0
0.4	30.1	28.0	29.0	29.0
0.5	30.0	31.0	32.0	31.0

Table 4.8: Variation of hardness with Cr addition for the Age-hardened alloy.

%Cr addition	1st HRB	2nd HRB	3rd HRB	Mean HRB
Control	19.0	15.0	20.0	18.0
0.1	20.0	21.0	22.0	21.0
0.2	24.0	25.0	26.0	25.0
0.3	34.0	31.0	32.0	32.3
0.4	37.0	33.0	36.0	35.3
0.5	41.0	42.0	43.0	42.0

Table 4.9: Variation of the Hardness with % manganese addition for the as-cast alloys.

%Mn addition	1st HRB	2nd HRB	3rd HRB	Mean HRB
Control	14.0	13.0	14.0	13.7
0.1	20.0	20.0	20.0	20.0
0.2	20.5	21.0	21.0	20.8
0.3	24.0	24.0	24.0	24.2
0.4	31.0	34.5	31.0	32.2
0.5	26.0	25.0	26.0	25.6

Table 4.10: Variation of the hardness with % manganese addition for the age-hardened alloys.

%Mn addition	1st HRB	2nd HRB	3rd HRB	Mean HRB
Control	19.0	15.0	20.0	18.0
0.1	20.0	22.0	24.0	22.0
0.2	29.0	30.0	25.0	28.0
0.3	31.0	29.0	30.0	30.0
0.4	40.0	41.0	39.0	40.0
0.5	30.0	29.0	31.0	30.0

Table 4.11: Variation of Hardness with % Manganese – Chromium (MnCr) addition for the as-cast alloys.

%MnCr addition	1st HRB	2nd HRB	3rd HRB	Mean HRB
Control	14.0	13.0	14.0	13.7
0.1Mn-0.1Cr	20.0	21.0	22.0	21.0
0.2Mn-0.2Cr	24.0	24.0	24.0	24.0
0.3 Mn-0.3Cr	27.0	28.0	28.0	27.7
0.4 Mn-0.4Cr	32.0	33.0	34.0	33.0
0.5 Mn-0.5Cr	30.0	31.0	31.0	30.7

Table 4.12: Variation of Hardness with % Manganese-Chromium (MnCr) addition for the age-hardened alloys.

%MnCr addition	1st HRB	2nd HRB	3rd HRB	Mean HRB
Control	19.0	15.0	20.0	18
0.1Mn-0.1Cr	24.0	21.0	24.0	23.0
0.2Mn-0.2Cr	31.0	27.0	28.0	28.7
0.3 Mn-0.3Cr	32.0	31.0	33.0	32.0
0.4 Mn-0.4Cr	45.0	44.0	40.0	43.0
0.5 Mn-0.5Cr	38.0	39.0	40.0	39.0

.

Table 4.13: Variation of the Impact Energies for % Chromium Addition for both as – cast and age – hardened alloys.

% Cr addition	As – cast Impact energy (Joule)	Age-hardened impact energy (Joule)
Control	29	60
0.1	39	82
0.2	11	38
0.3	10	36
0.4	7.0	15
0.5	5.0	8.0

Table 4.14: Variation of the Impact Energies for % Manganese Addition for the as – cast and age – hardened alloys.

% Mn addition	As–cast Impact energy (Joule)	Age-hardened impact energy (Joule)
Control	29	60
0.1	17	42
0.2	15	27
0.3	13	20
0.4	11	16
0.5	10	16

Table 4.15: Variation of the Impact Energies for %Manganese-Chromium (MnCr) addition for the as–cast and age–hardened alloys.

%MnCr addition	As – cast Impact energy (Joule)	Age-hardened impact energy (Joule)
Control	29	60
0.1Mn-0.1Cr	23	56
0.2 Mn-0.2Cr	18	48
0.3 Mn-0.3Cr	16	46
0.4 Mn-0.4Cr	15	39
0.5 Mn-0.5Cr	10	34

Table 4.16: Corrosion Rate of as-cast Al-Si-Fe-Cr alloys in 0.5M HCl Over exposure time (hours).

% Cr addition	Corrosion rate in mpy x10^3									
	48hrs	96hrs	144hrs	192hrs	240hrs	288hrs	336hrs	384hrs	432hrs	480hrs
Control	1.174	0.700	0.540	0.443	0.392	0.339	0.332	0.301	0.277	0.257
0.1	1.088	0.631	0.517	0.422	0.372	0.332	0.323	0.294	0.271	0.251
0.2	1.091	0.573	0.472	0.396	0.355	0.308	0.309	0.285	0.262	0.247
0.3	1.159	0.662	0.534	0.424	0.375	0.314	0.306	0.277	0.255	0.237
0.4	0.855	0.515	0.424	0.326	0.298	0.254	0.277	0.256	0.240	0.228
0.5	0.726	0.511	0.430	0.344	0.299	0.262	0.276	0.251	0.234	0.219

Table 4.17: Corrosion Rate of aged-hardened Al-Si-Fe-Cr alloys in 0.5M HCl Over the exposure time (hours).

% Cr addition	Corrosion rate in mpy x10^3									
	48hrs	96hrs	144hrs	192hrs	240hrs	288hrs	336hrs	384hrs	432hrs	480hrs
Control	1.451	0.831	0.592	0.460	0.380	0.325	0.287	0.259	0.235	0.216
0.1	1.212	0.658	0.508	0.384	0.316	0.264	0.264	0.242	0.222	0.211
0.2	1.322	0.725	0.539	0.420	0.351	0.304	0.270	0.242	0.225	0.208
0.3	1.258	0.745	0.540	0.420	0.349	0.302	0.267	0.242	0.220	0.203
0.4	0.919	0.501	0.398	0.319	0.288	0.246	0.249	0.227	0.209	0.195
0.5	0.833	0.480	0.394	0.312	0.287	0.244	0.240	0.226	0.208	0.195

Table 4.18: Corrosion rate of as-cast Al-Si-Fe-Mn alloys in 0.5M HCl Over the exposure time (hours).

% Mn addition	Corrosion rate in mpy x10^3									
	48hrs	96hrs	144hrs	192hrs	240hrs	288hrs	336hrs	384hrs	432hrs	480hrs
Control	1.174	0.700	0.540	0.443	0.392	0.339	0.332	0.301	0.277	0.257
0.1	1.304	0.716	0.577	0.454	0.395	0.351	0.316	0.291	0.269	0.249
0.2	1.174	0.591	0.493	0.383	0.341	0.303	0.311	0.286	0.264	0.246
0.3	1.295	0.815	0.597	0.469	0.399	0.347	0.311	0.284	0.259	0.241
0.4	1.304	0.716	0.577	0.454	0.380	0.332	0.296	0.269	0.252	0.231
0.5	1.056	0.625	0.579	0.397	0.341	0.301	0.288	0.258	0.2 49	0.217

Table 4.19: Corrosion Rate of aged-hardened Al-Si-Fe-Mn alloys in 0.5M HCl over the exposure time (hours).

% Mn addition	Corrosion rate in mpy x10^3									
	48hrs	96hrs	144hrs	192hrs	240hrs	288hrs	336hrs	384hrs	432hrs	480hrs
Control	1.451	0.831	0.592	0.460	0.380	0.325	0.287	0.259	0.235	0.216
0.1	1.264	0.805	0.571	0.447	0.373	0.321	0.285	0.257	0.233	0.215
0.2	1.188	0.734	0.555	0.442	0.357	0.309	0.281	0.254	0.227	0.209
0.3	0.955	0.571	0.446	0.347	0.307	0.258	0.265	0.240	0.219	0.207
0.4	1.285	0.710	0.509	0.398	0.334	0.290	0.259	0.235	0.215	0.200
0.5	1.256	0.648	0.507	0.394	0.336	0.286	0.254	0.232	0.210	0.194

Table 4.20: Corrosion Rate of as-cast Al-Si-Fe-MnCr alloys in 0.5M HCl Over the exposure time (hours).

% MnCr addition	Corrosion rate in mpy x10^3									
	48hrs	96hrs	144hrs	192hrs	240hrs	288hrs	336hrs	384hrs	432hrs	480hrs
Control	1.174	0.700	0.540	0.443	0.392	0.339	0.332	0.301	0.277	0.257
0.1Mn-0.1Cr	1.329	0.803	0.607	0.480	0.405	0.354	0.317	0.291	0.270	0.248
0.2 Mn-0.2Cr	1.307	0.747	0.577	0.454	0.387	0.336	0.304	0.279	0.258	0.241
0.3Mn-0.3Cr	1.292	0.722	0.567	0.478	0.398	0.343	0.306	0.277	0.251	0.233
0.4Mn-0.4Cr	1.196	0.601	0.404	0.333	0.294	0.253	0.269	0.248	0.230	0.218
0.5Mn-0.5Cr	1.044	0.515	0.424	0.326	0.340	0.289	0.283	0.255	0.228	0.217

Table 4.21: Corrosion Rate of aged-hardened Al-Si-Fe-MnCr alloys in 0.5M HCl Over the exposure time (hours).

%MnCr addition	Corrosion rate in mpy x10^3									
	48hrs	96hrs	144hrs	192hrs	240hrs	288hrs	336hrs	384hrs	432hrs	480hrs
Control	1.451	0.831	0.592	0.460	0.380	0.325	0.287	0.259	0.235	0.216
0.1Mn-0.1Cr	1.257	0.772	0.542	0.426	0.356	0.309	0.275	0.251	0.229	0.211
0.2 Mn-0.2Cr	1.212	0.658	0.508	0.396	0.336	0.297	0.265	0.245	0.225	0.208
0.3Mn-0.3Cr	1.343	0.782	0.546	0.424	0.351	0.301	0.265	0.238	0.216	0.203
0.4Mn-0.4Cr	1.239	0.766	0.533	0.416	0.342	0.295	0.258	0.233	0.210	0.194
0.5Mn-0.5Cr	0.863	0.491	0.428	0.342	0.293	0.259	0.235	0.215	0.198	0.184

CHAPTER FIVE

5.0 SUMMARY

From the experimental results, the mechanical properties; tensile properties, hardness of the Al-Si-Fe alloys produced showed an improvement for all levels of the % Cr, Mn, and MnCr additions in the as-cast condition. But a decrease in impact energy of the alloys was observed. However, further improvement in the tensile strength, hardness and impact energy were noticed after age-hardening the alloys. For the corrosion resistance of these alloys in 0.5M HCl solution at 28^0C, the corrosion rate decreased as the percentage of additions were increased respectively with exposure time in the as-cast condition. Age-hardening of the alloys shows that there was significant resistance of the alloys to corrosion for all levels of additions and exposure time considered. However, the alloys with improved mechanical properties and corrosion resistance can be used in automobile industry as oil pan, flywheel and rear-axle housings, cranks cases, transmission cases, clutch components and in aerospace and aviation industry as tankage for storage of liquid fuels and oxidizers, airframes, engines, propellers, accessories, etc.

5.1 Conclusion

From the results obtained in this research it can be concluded that

1. Addition of Cr, Mn separately and simultaneously to Al-Si-Fe alloy improved the tensile properties and the hardness and corrosion

resistance in 0.5M HCl solution in both as-cast and the age-hardened conditions subject to a maximum of 0.5% (Mn and Cr) addition.

2. Heat-treatment (Age-hardening) improves the mechanical properties and corrosion resistance of the alloys in 0.5M HCl solution at room temperature.
3. While the addition of Mn and Cr lowers the impact resistance of the as-cast alloy but it improves after age-hardening and simultaneous addition of these elements is better than individual additions in terms of mechanical properties investigated and corrosion resistance of the alloys.

5.2 Recommendations

Based on the research output obtained, and analysis, the followings are recommended:

1. Typical automobile and aerospace prototype parts should be produced out of alloy compositions with optimum mechanical properties and corrosion resistance.
2. The fatigue properties of Al-Si-Fe alloys with Cr, Mn, and MnCr should be investigated for purpose of application in cyclic loading situation.
3. The effect of varying ageing temperatures and time on the mechanical properties of the alloys should be looked into.
4. The effects of heat treatment and different quenching media on the mechanical properties and corrosion characteristics of the produced alloys should be investigated.

5. Scanning Electron Microscopy (SEM), Transmission Electron Microscopy (TEM) and other equipments should be used to examine the microstructures for better understanding of the concept of dislocation and grain boundary phenomenon.

REFERENCES

Allen, D.K. (1979): Metallurgy Theory and Practice, American Technical Society, Chicago

Avner, S.H. (1974): Introduction to Physical Metallurgy 2nd Edition McGraw – Hill Inc. London, Pp 481 - 497

Barer, R.D. and Peters, B.F., (1974): Why Metals Fail, 3rd Impression, Gordon and Breach, Science Publishers, INC, New York.

Brumbough, James E. (1979): Welders Guide 2nd edition, 7th reprinted copy of Theodore Audel and Co. Indianapolis, Indiana. Pp 777 – 786

Carter, V.E. (1977): Metallic Coatings for corrosion control, Butterworths and Co. Publishers Ltd.

Chalmers, Bruce (1964): Principles of Solidification, Robert E Krieger publishing company Huntington, New York. Pp 12

Datsko, J. (1966): Materials Properties and Manufacturing Processes John Wiley and Son Publishers, New York

Fontana, M.G and Greene, N.D. (1987): Corrosion Engineering McGraw-Hill book Company. New York. Pp 8 – 29

Gayle, F.W and Vadersande, J.B. (1986): Proceedings of International conferences on aluminium alloy their physical and mechanical properties Vol. 727, Warley engineering materials advisory service.

George E. Dieter (1981): Mechanical Metallurgy, 2nd Edition, McGraw-Hill International Book Company, London. Pp 190 – 198

Ghosh, K.S, Das.K. and Chatterjee, U.K. (2004): Studies of the microstructural changes upon retrogression and reageing (RRA) treatment to 8090 Al-Li-Cu-Mg-Zr alloy, *Journals of materials science and technology Vol. 20, Pp 825-834*

Greenfield P. (1971): M & B Monographs, Mechanical Engineering, Stress Corrosion Failure, published by Mills & Boon Ltd, London.

Hansen, V., Karlsen, O.B., Langsrud, Y. and Gjonnes, J. (2004): Precipitates, zones and transitions during ageing of Al-Zn-Mg-Zr 7000 series alloys, *Journal of Materials Science and Technology, Vol. 20, Pp 185-193*

Idenyi, N.E. and Neife S.I. (2005):, The Corrosion behaviour of Aluminium base alloys in Caustic soda (NaOH) media. *Journal of Corrosion Science and Technology, Vol. 3, Pp 9 – 13*

International Aluminium Institute (IAI) 2000, www.world-Aluminium.org Internet link.

International Aluminium Institute (IAI) 2006, www.world-Aluminium.org Internet link.

Internet link (2002): Development in Aluminium Heat-treating, www.Secant.net/answers_view_article.php?article.

Internet link (2007): Aluminium Alloys-Effects of Alloying Elements, www.key-to-metals.com

Internet link (2007): Heat-treating of Aluminium and Aluminium alloys, www.key-to-metals.com/atricle7.htm

Internet link (2007): Precipitation strengthening, Wikipedia, www.answers.com/topic/precipitation-strengthening.

Kenneth G. Budinski (1999): Engineering Materials, Properties and Selection 5th Edition Prentice Hall. Pp 518 – 529

Markandeya.R, Nagarjuna, S. and Sarma.D.S. (2004): Precipitation hardening of Cu-Ti-Zr alloys, *Journals of materials science and technology Vol. 20 Pp 849-858*

Metal Hand Book (1966): Properties and Selection of metals ASM USA. Pp 866 – 888

Metal Hand Book (1975): Heat-treating, Cleaning and Finishing, 8th Edition Vol. 2, American Society of Metal (ASM) Metals Park Ohio 1975, USA

Metal Hand Book (1979A): Properties and Selection of Non-ferrous alloys and pure metals, ASM USA.

Metal Hand Book (1979B): Atlas of Microstructures of Metal and Alloys, ASM Ohio USA.

Metals Hand Book (1981): Heat-treating, 9th edition, Volume 4, American Society of Metals (ASM), USA.

Michael J. Kroes and James R. Rardon (1993): Aircraft Basic Science, 7th Edition Published by Glencoe/McGraw – Hill, New York.

Nwajagu C.O. (1994): Foundry Theory and Practice, ABC Publishers Ltd, Enugu, Nigeria.

Odutola, M.F.A. (2005):, The effects of Corrosion and Measures taken to control Corrosion related failures in the aviation industry. Paper presented

during the Nigerian Corrosion Association (NICA) National Conference held in Jos.

Pascoe K.J. (1962): An Introduction to the properties of Engineering Materials, Blackie and Son ltd, London and Glasgow. Pp 83 – 85

Quraishi, M.A. and Ansanri, F.A., (2003): Corrosion Inhibition by Fatty acid Triazoles for mild Steel in formic acid. *Journal of Applied Electro Chemistry, 33:233, Netherlands.*

Quraishi, M.A. and Tamal, (2000): CAMT – A New and Eco-friendly acidizing corrosion inhibitors, *corrosion 56. 156. USA.*

Rajan T.V., Sharma C.P. and Sharma, A. (1988): Heat Treatment Principles and Techniques, Published by Prentice Hall of India Private Ltd. New Delhi. Pp 314 – 338.

Rhines, F.N., (1956): Phase Diagrams in Physical Metallurgy, McGraw – Hill Book Company.

Rollason E.C. (1964): Metallurgy for Engineers, Reprinted Edition, Richard Clay and Company ltd., Bungay. Pp 304 – 306.

Smith William F. (1981): Structures and properties of Engineering Alloys. McGraw-Hill book Company, New York. Pp 168 – 176

Thompson, S., Cockcroft, S.L. and Wells, M.A. (2004): Advanced Light metals casting development: Solidification of aluminium alloy A356, *Journal of Materials Science and Technology, Vol. 20, Pp 194-200*

William D.C. (1997): Materials Science and Engineering: An Introduction John Wiley and Sons INC., New York.

Yaro S.A. and Aigbodion V.S. (2006): The effect of Copper addition on the corrosion behaviour of As-cast Al – Si – Fe alloy in acidic media. *Journal of Corrosion Science and Technology.*

Yaro, S.A., Aigbodion, V.S., and Mohammed, Y.O. (2006): The Effect of Copper addition on the mechanical properties of Al-Si-Fe alloy. International Research, *Journal in Engineering, Science and Technology Vol.3, No2, Pp 32 – 39.*

Yawas, D.S., (2005): Assessment of suitability of some vegetable based oils and plant extracts as corrosion inhibitors, 2nd Ph.D seminar, Department of Mechanical Engineering, Ahmadu Bello University, Zaria. Pp 4-6.

APPENDIX A; MICROGRAPHS (PLATES)

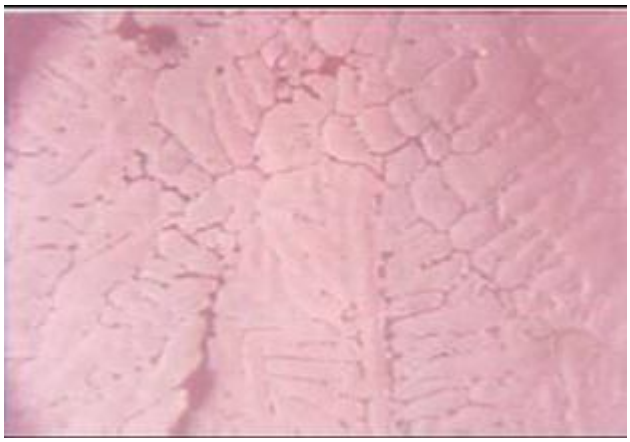


Plate 1: Microstructure of As-cast Al- Si-Fe Alloy X 100
Consist of interdentritic structure of silicon eutectic in matrix of Al-solid solution.

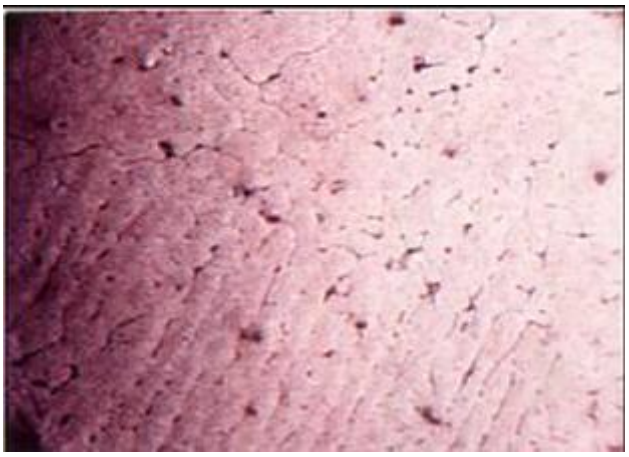


Plate 2: Microstructure of As-cast Al- Si-Fe- 0.1% Cr Alloy X 125
Network consists of $CrAl_6$ precipitates within the matrix of Al-Solid solution.

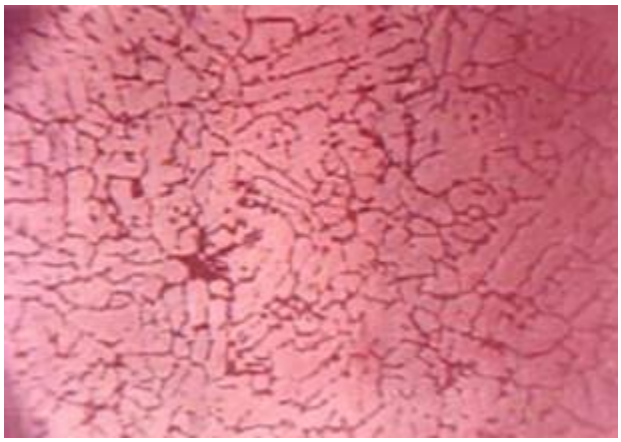


Plate 3: Microstructure of As-cast Al- Si-Fe- 0.2% Cr Alloy X 100
Finer interdentritic network with dissolved $CrAl_6$ particles



Plate 4: Microstructure of As-cast Al- Si-Fe- 0.3% Cr Alloy X 100
As in plate 3 but more fine structure

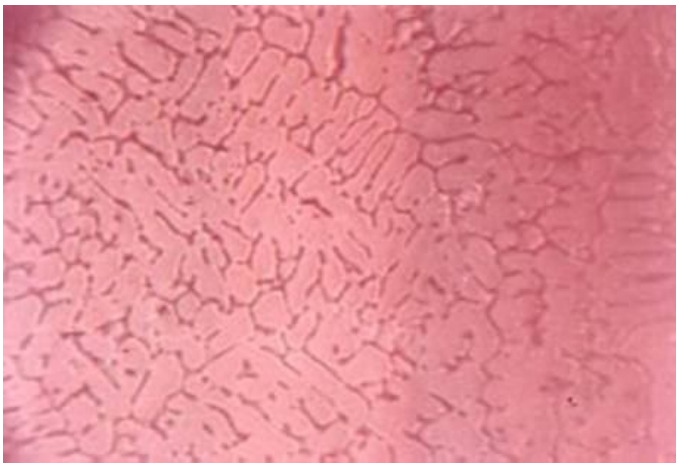


Plate 5: Microstructure of As-cast Al- Si-Fe- 0.4% Cr Alloy X 100 Smaller interdentritic structure of silicon eutectic with little or no particles

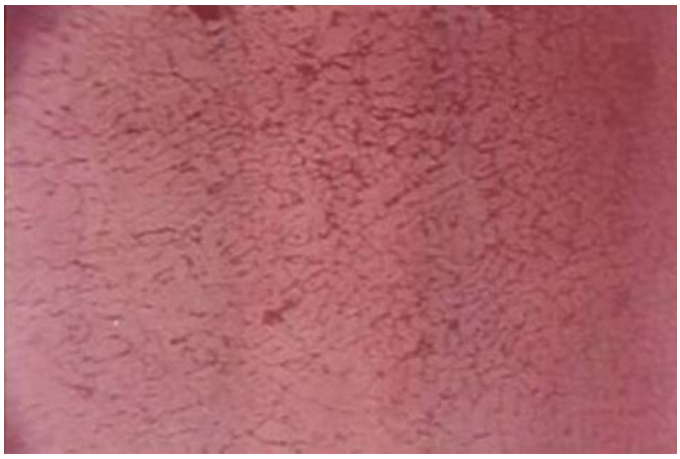


Plate 6: Microstructure of As-cast Al- Si-Fe- 0.5% Cr Alloy X 100 Fine constituent network of $CrAl_6$ with smaller and many softer boundaries

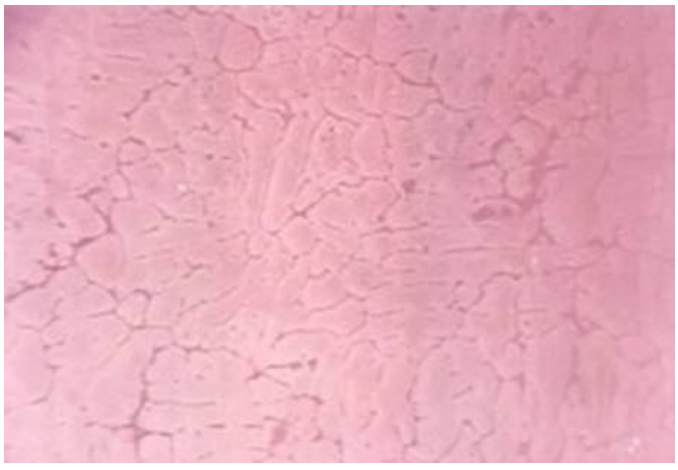


Plate 7: Microstructure of As-cast Al- Si-Fe- 0.1% Mn Alloy X 100 Little change in structure as compared to plate 1, but finer network

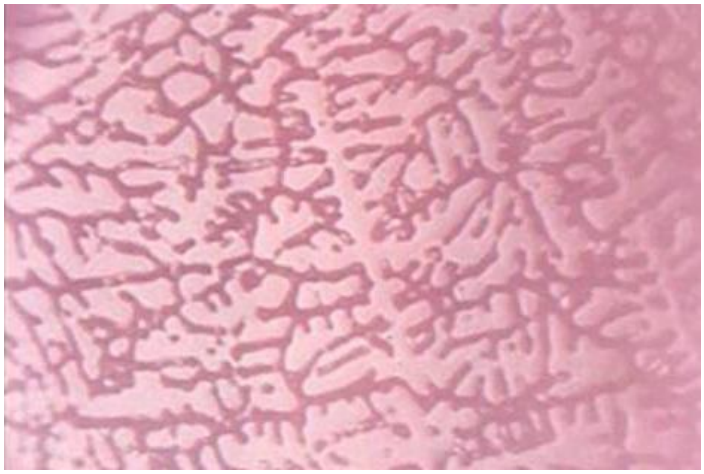


Plate 8: Microstructure of As-cast Al- Si-Fe- 0.2% Mn Alloy X 100 Structure consist of a network of silicon particles in a divorced interdendritic Al-Si-Fe eutectic and particles of $(FeMn)_3SiAl_{12}$ phase

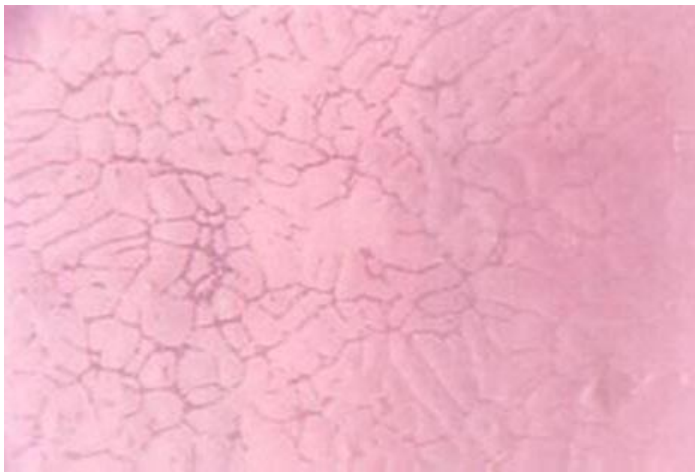


Plate 9: Microstructure of As-cast Al- Si-Fe- 0.3% Mn Alloy X 100 Interdendritic cells are thinner and less angular as compared to plate 8.

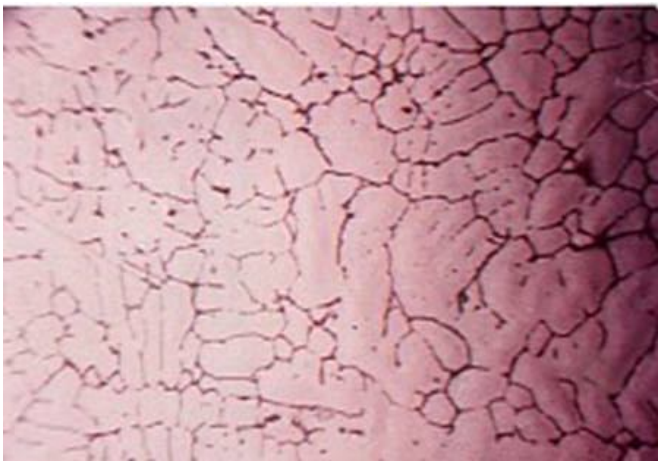


Plate10: Microstructure of As-cast Al- Si-Fe- 0.4% Mn Alloy X 100 Bond network of $(FeMn)_3SiAl_{12}$ particles at grain boundaries.

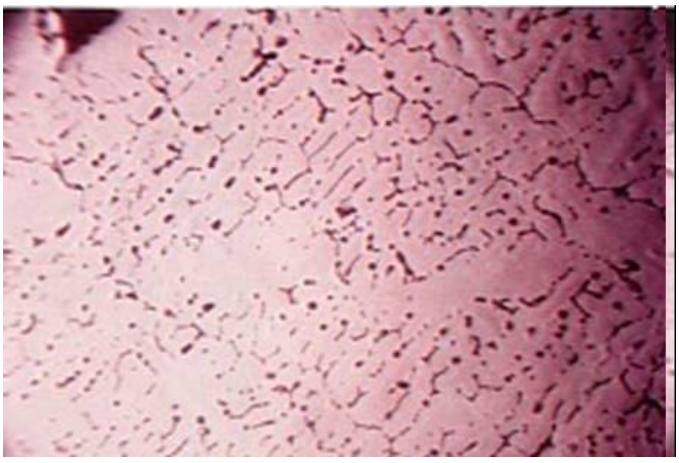


Plate11: Microstructure of As-cast Al- Si-Fe- 0.5% Mn Alloy X 100 More particles formed .

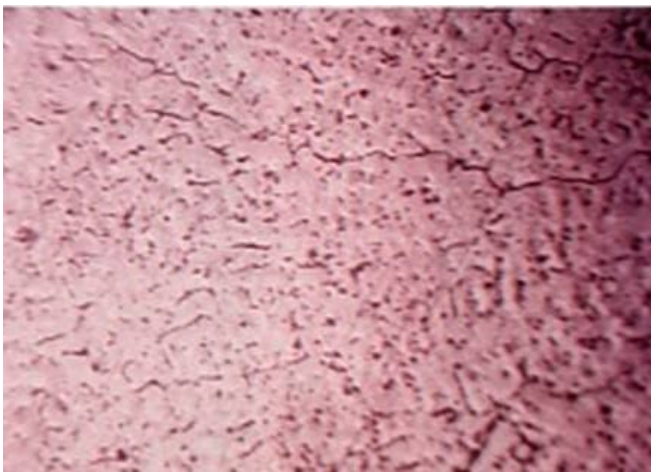


Plate12: Microstructure of As-cast Al- Si-Fe- 0.1% Mn- 0.1%Cr Alloy X 100 The structure consist of eutectic silicon (gray constituent) and some light particles, probably are Fe_3SiAl_{12}, in a matrix of Al-Solid solution.



Plate13: Microstructure of As-cast Al- Si-Fe- 0.2% Mn- 0.2%Cr Alloy X 125 Same as plate 12, but more grain boundaries formed

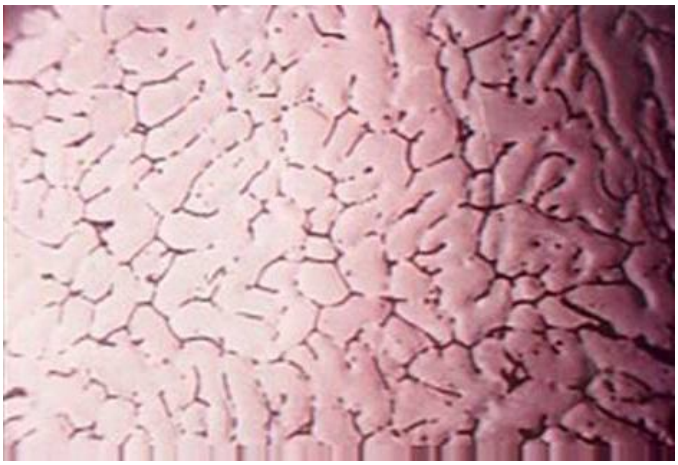


Plate14: Microstructure of As-cast Al- Si-Fe- 0.3% Mn- 0.3%Cr Alloy X 125 More interdendritic network and grain boundaries.



Plate15: Microstructure of As-cast Al- Si-Fe- 0.4% Mn- 0.4%Cr Alloy X 125 Fineness of structure results with dissolved $MnCrAl_6$ particles.

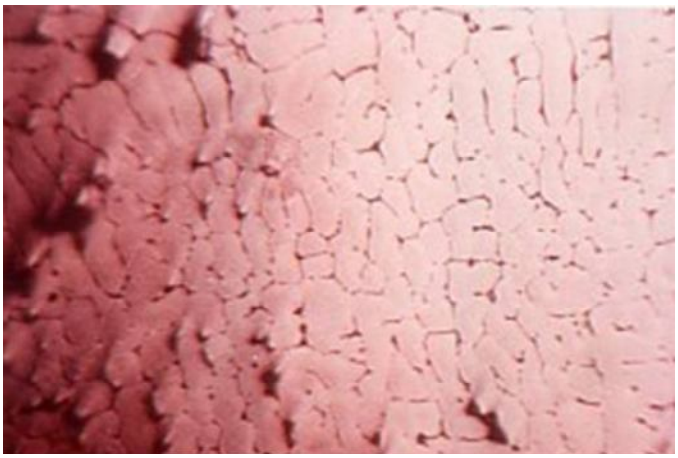


Plate16: Microstructure of As-cast Al- Si-Fe- 0.5% Mn- 0.5%Cr Alloy X 125 Similar to plate 9, but more precipitate at grain boundaries.

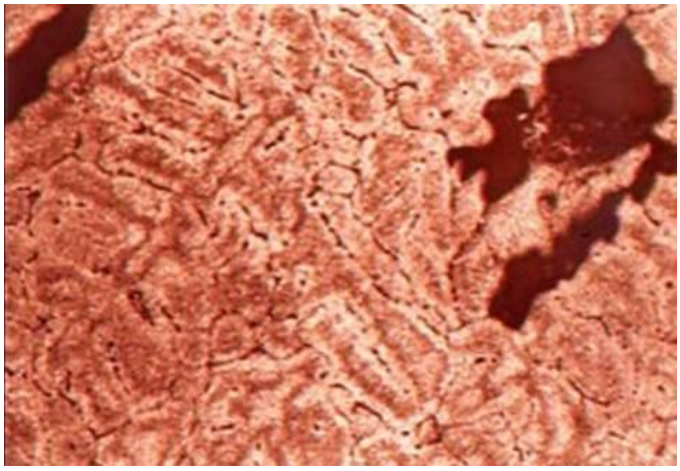


Plate17: Microstructure of Age-Hardened Al- Si-Fe Alloy (Control) X 100
Breakdown of interdendritic structure of Silicon eutectic and $FeAl_6$ and a more fine grain particles with the matrix (as compared to as-cast microstructure).

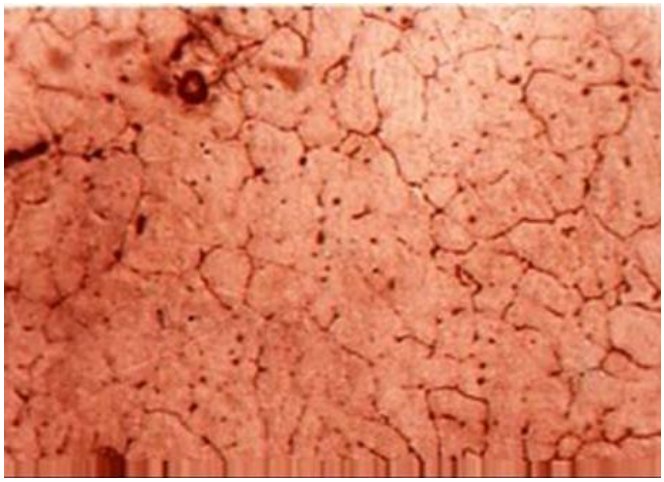


Plate18: Microstructure of Age-Hardened Al- Si-Fe- 0.1% Cr Alloy X 100
Interdendritic network made up of particles of $CrAl_7$, Fe_3SiAl_{12} and $FeAl_6$

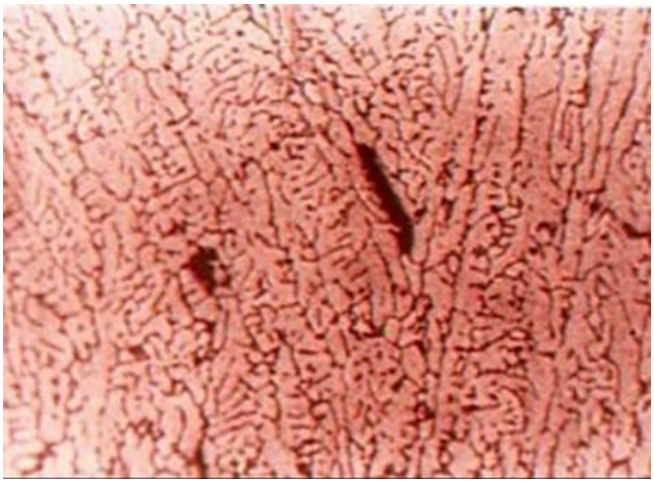


Plate19: Microstructure of Age-Hardened Al- Si-Fe- 0.2% Cr Alloy X 100
Interdendritic network, which shows very little undissolved CrSi remained after solution heattreatment.

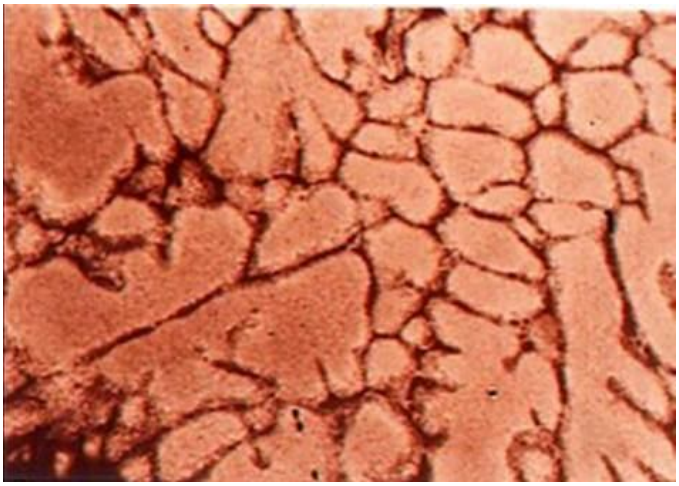


Plate20: Microstructure of Age-Hardened Al- Si-Fe- 0.3% Cr Alloy X 100.
The structure consists of equiaxed dendrites of aluminium with a fine precipitates of $CrAl_3$ (dark) in the dendrite and at dendrite boundaries.

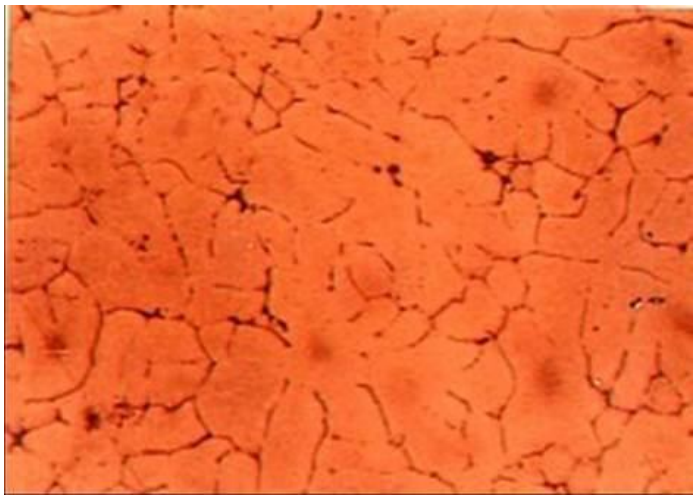


Plate21: Microstructure of Age-Hardened Al- Si-Fe- 0.4% Cr Alloy X 100
The structure shows a breakdown in the dendrite boundaries and more finer structure formed.

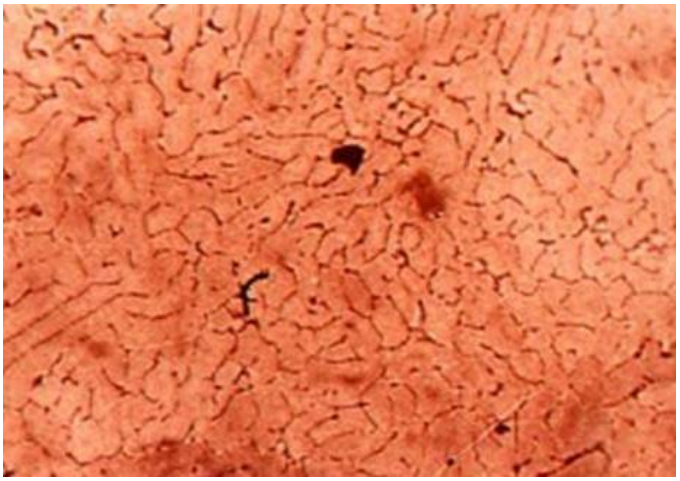


Plate22: Microstructure of Age-Hardened Al- Si-Fe- 0.5% Cr Alloy X 100
Fine structure; almost all of the eutectic $CrAl_2$ precipitates has dissolved.



Plate23: Microstructure of Age-Hardened Al- Si-Fe- 0.1% Mn Alloy X 100
Little breakdown of interdendritic network of Silicon eutectic in Al- matrix.

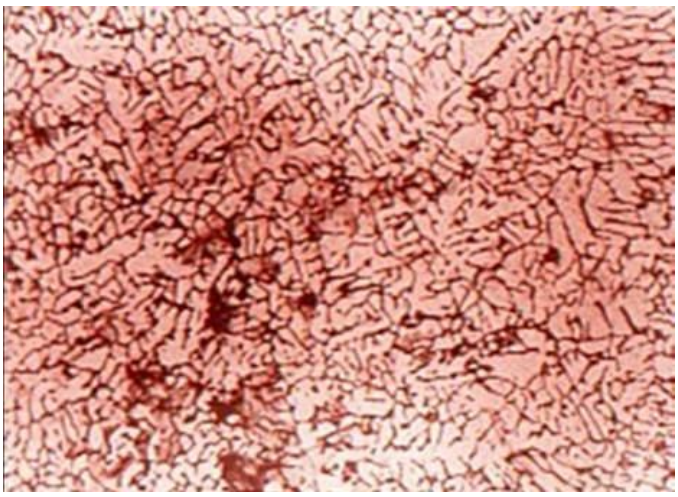


Plate24: Microstructure of Age-Hardened Al- Si-Fe- 0.2% Mn Alloy X 100
Dendrites of Al-solid solution .Other constituents are interdendritic network of Silicon(dark-grey) and $(FeMn)_3SiAl_{12}$ script.

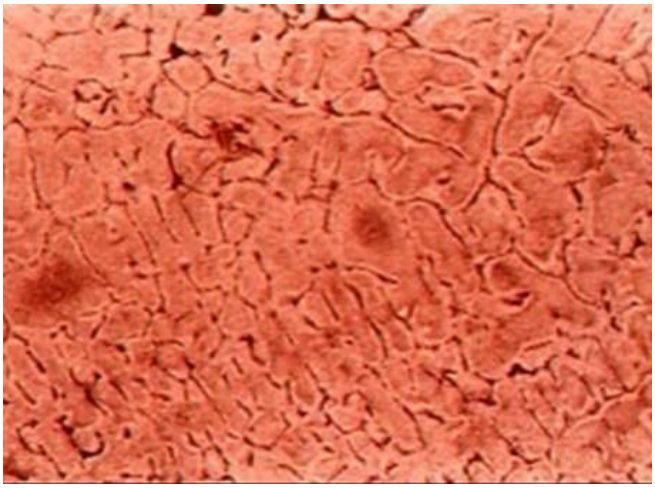


Plate25: Microstructure of Age-Hardened Al- Si-Fe- 0.3% Mn Alloy X 100
Interdendritic network of Silicon and $(FeMn)_3SiAl_{12}$ script become more.

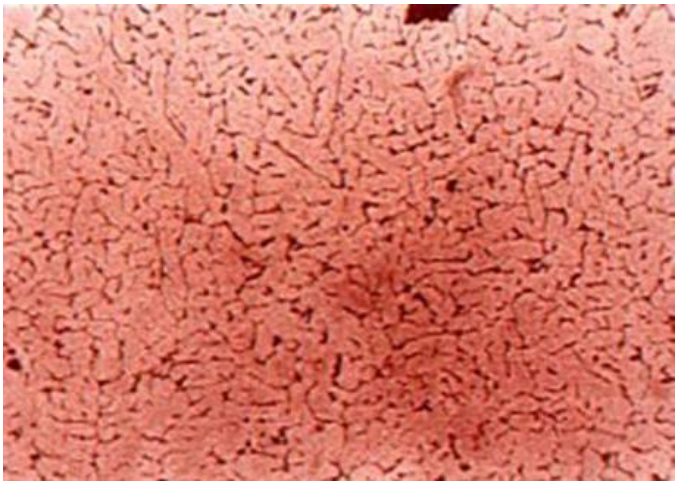


Plate26: Microstructure of Age-Hardened Al- Si-Fe- 0.4% Mn Alloy X 100
Network becomes finer structures consisting of Manganese-rich precipitates within the matrix of Al-Si-Fe constituent.

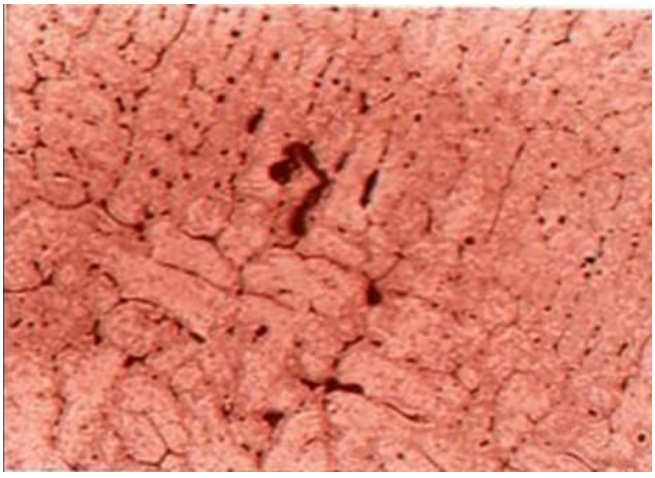


Plate27: Microstructure of Age-Hardened Al- Si-Fe- 0.5% Mn Alloy X 100
There is coarse stucture with particle of Mn predominantly forming more softer phases.

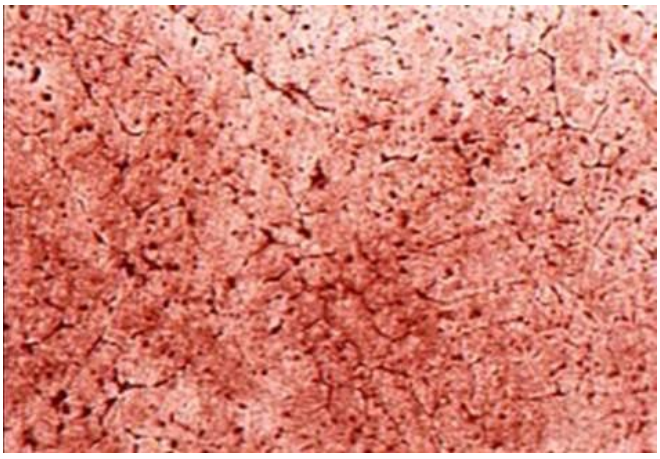


Plate28: Microstructure of Age-Hardened Al- Si-Fe- 0.1% Mn-0.1% Cr Alloy X 100
Fine constituent of $CrAl_2$, $(Fe,Mn)_3SiAl_{12}$ and interdendritic network of Silicon.

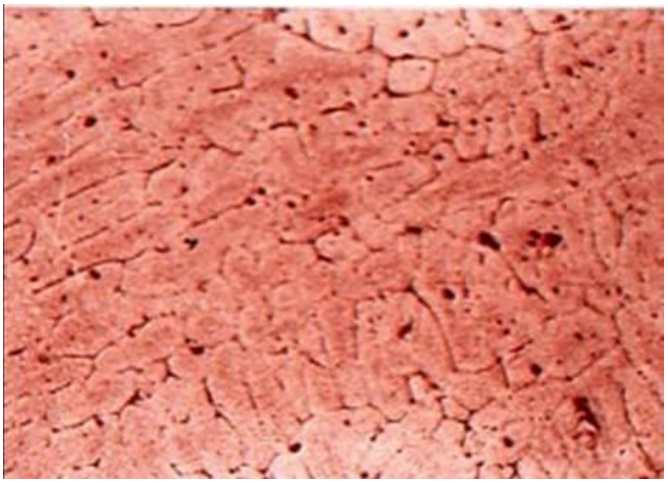


Plate29: Microstructure of Age-Hardened Al- Si-Fe- 0.2% Mn-0.2% Cr Alloy X 100 Structure shows a fairly even pattern of fine particles of $CrAl_2$ and $(FeMn)_3SiAl_{12}$ precipitate in the Al- grains, and slightly larger particles of the precipitate at grain boundaries.



Plate30: Microstructure of Age-Hardened Al- Si-Fe- 0.3% Mn-0.3% Cr Alloy X 100 Network becomes bond.

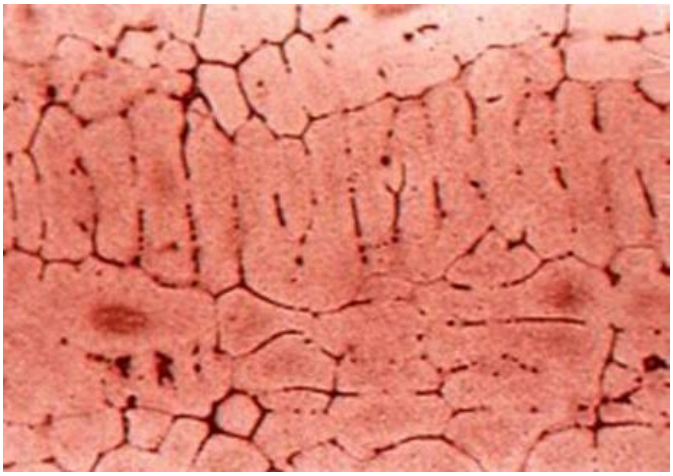


Plate31: Microstructure of Age-Hardened Al- Si-Fe- 0.4% Mn-0.4% Cr Alloy X 100 Larger network of Al- grains, enlarged grain boundaries and more precipitate of $CrAl_2$ and $(FeMn)_3SiAl_{12}$ formation.

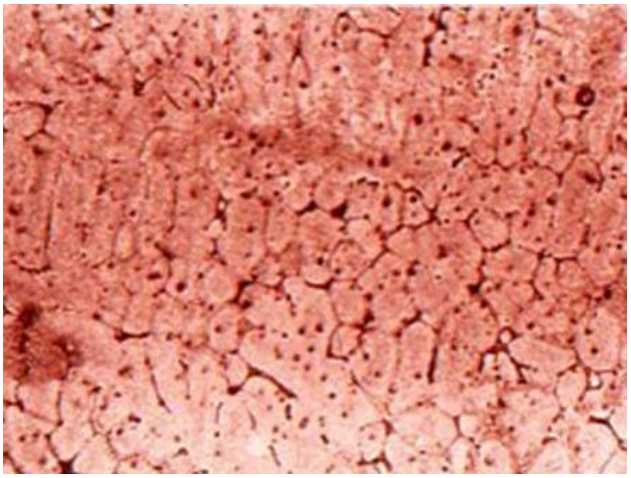


Plate32: Microstructure of Age-Hardened Al- Si-Fe- 0.5% Mn-0.5% Cr Alloy X 100 Excess Mn and Cr results in softer phase of the network (account for drop in the mechanical properties).

APPENDIX B; GRAPHS (FIGURES)

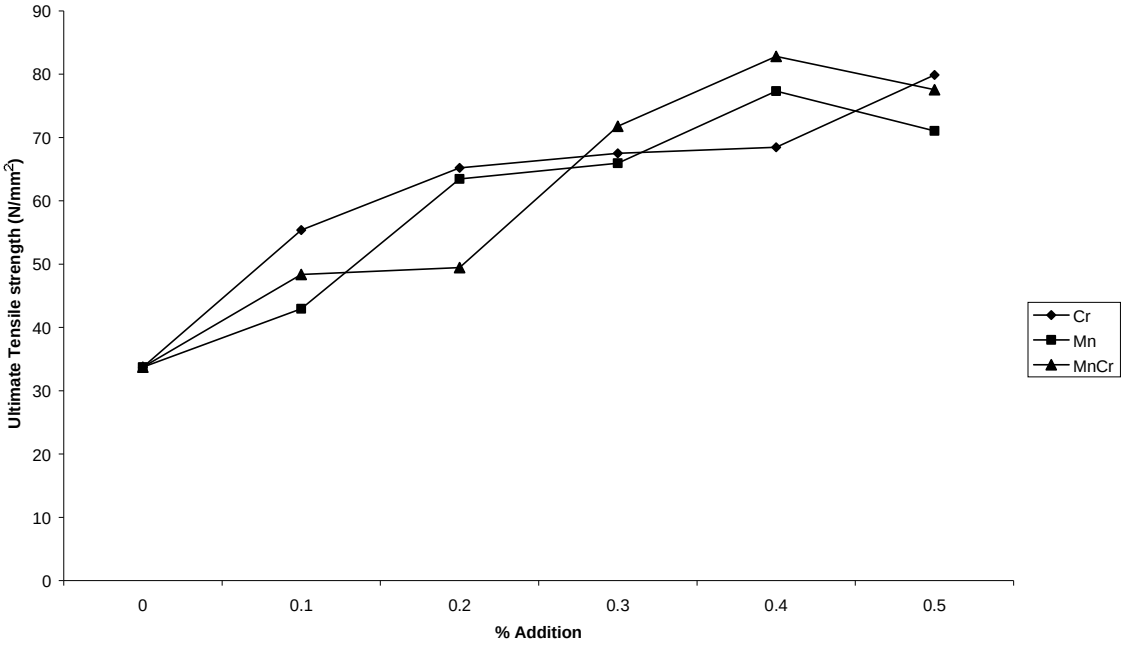


Figure 1: **Variation of Ultimate Tensile Strength (UTS) with % additions (Cr, Mn, MnCr) for As-cast conditions**

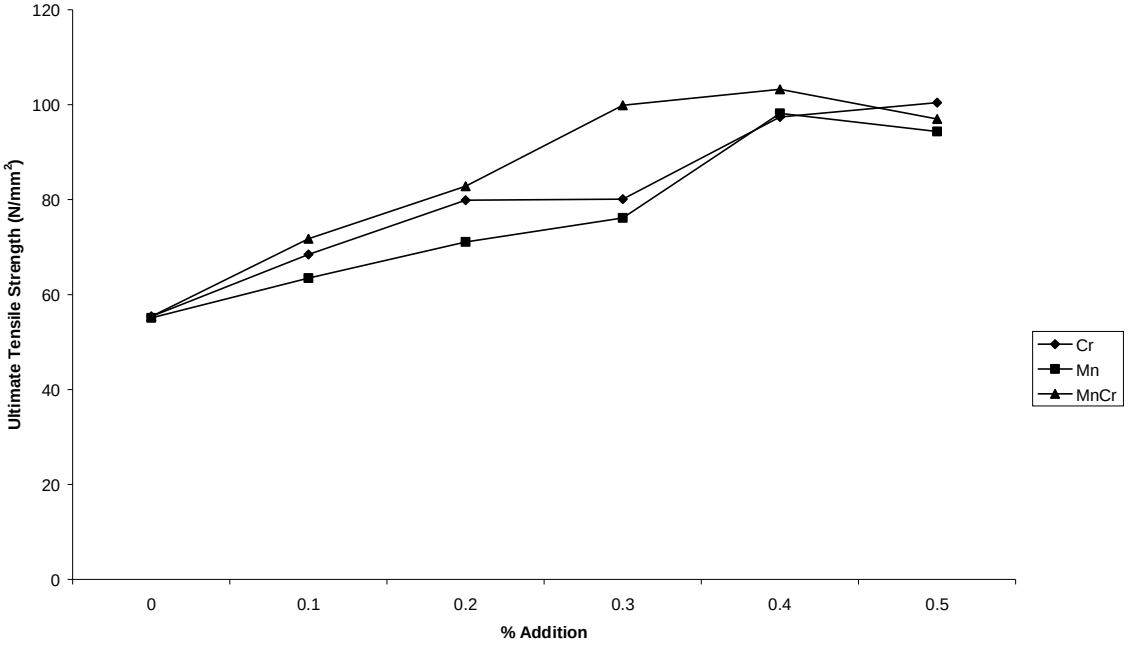


Figure 2: **: Variation of Ultimate Tensile Strength (UTS) with % addition (Cr,Mn, MnCr) for Age-hardened Conditions**

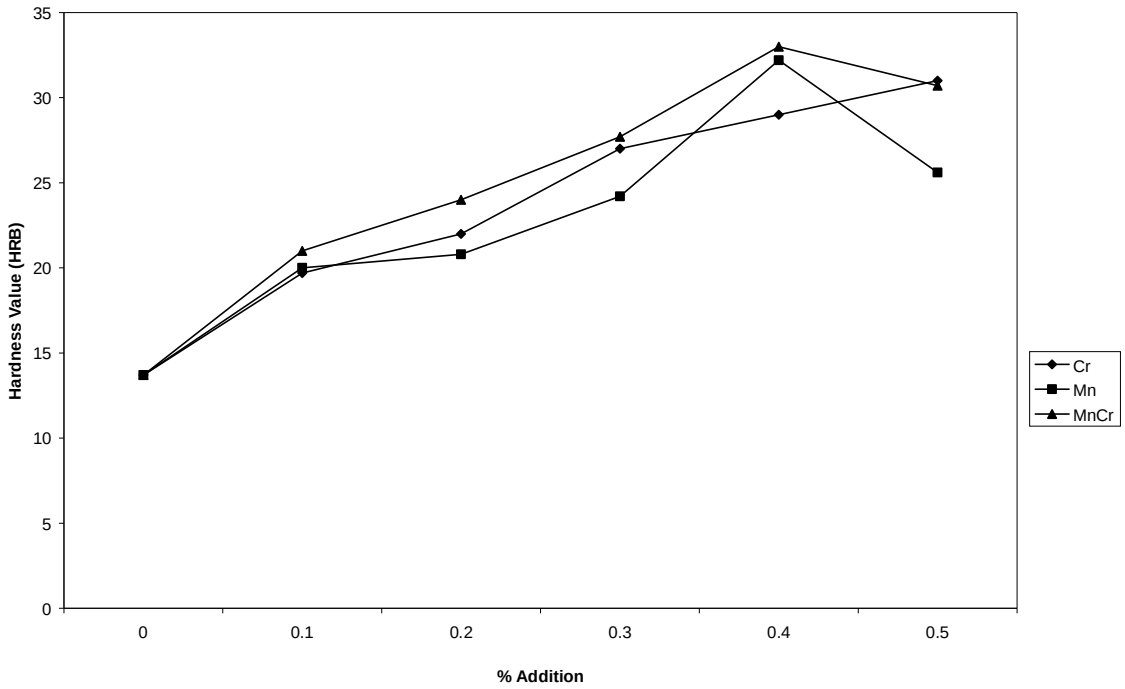


Figure 3: **Variation of Hardness Value with % Additions for As-cast Conditions**

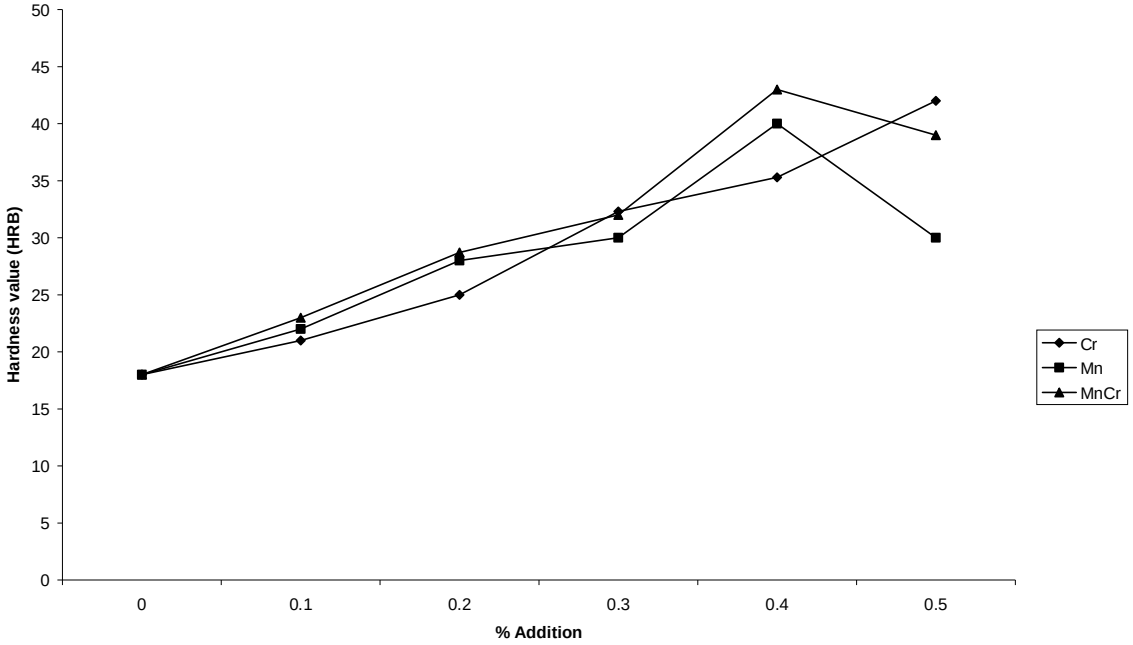


Figure 4: **Variation of Hardness value with % Additions (Cr, Mn, MnCr) for Age-hardened Conditions**

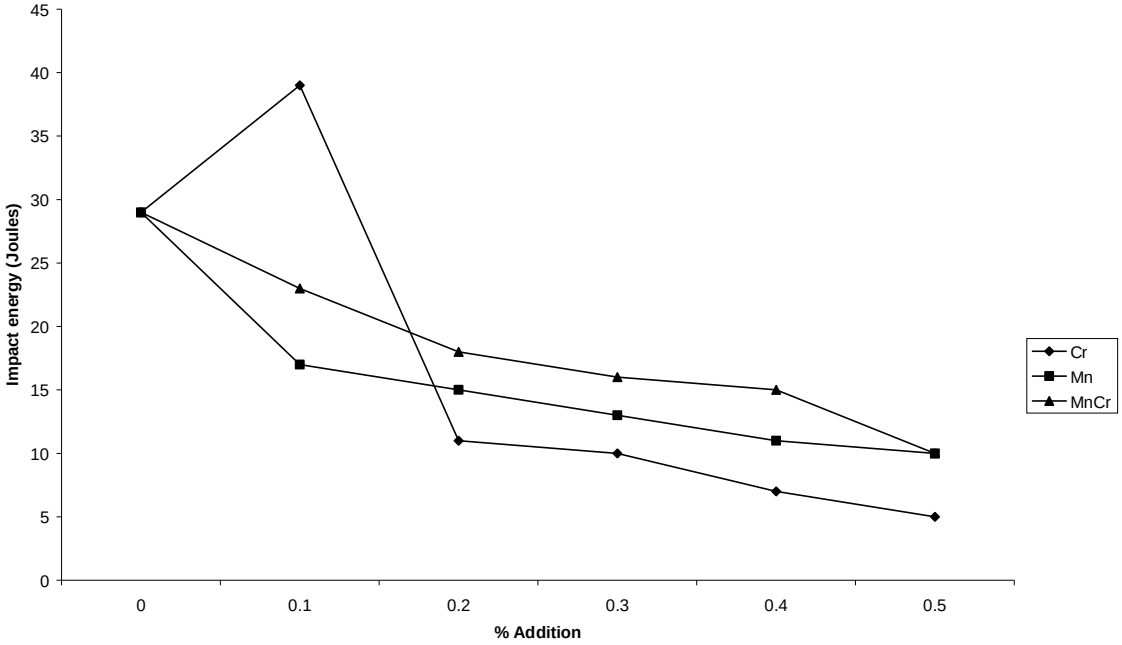


Figure 5: Variation of Impact Energy with % additions (Cr, Mn and MnCr) for As-cast conditions

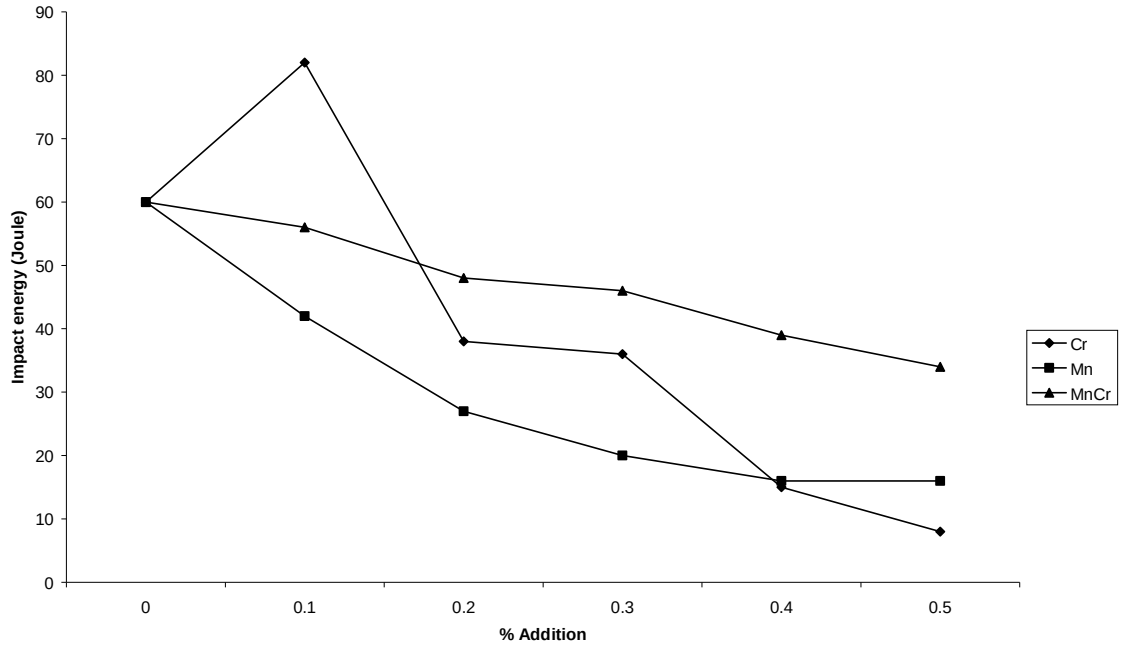


Figure 6: Variation of Impact energy with %Additions (Cr, Mn, MnCr) for Age-hardened conditions

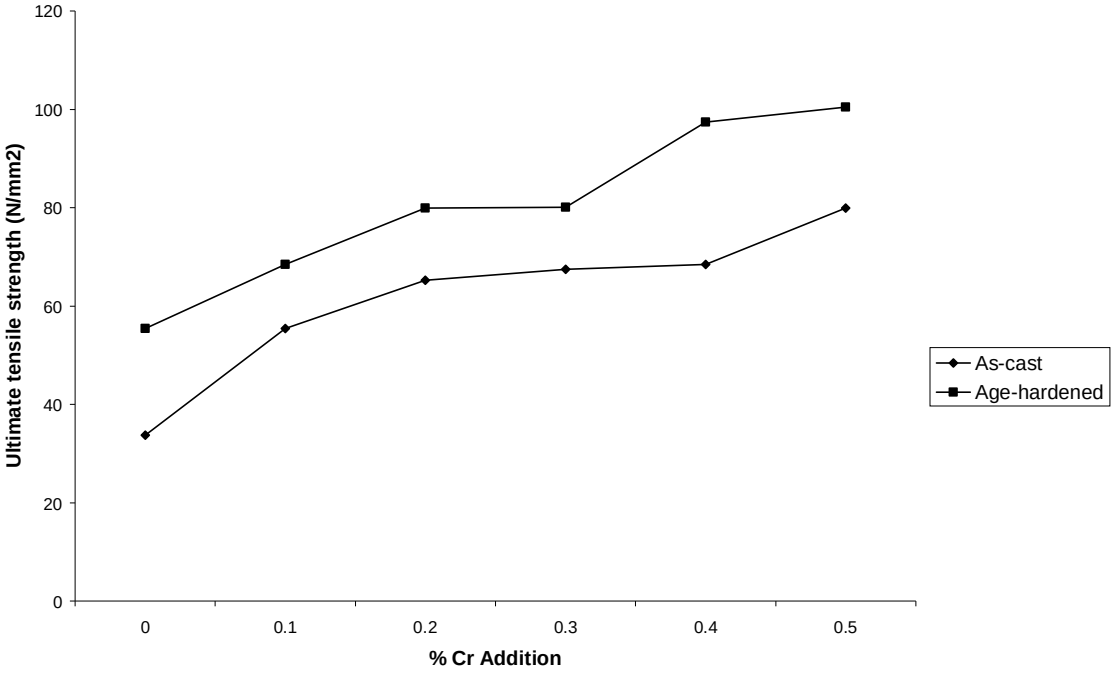


Figure 7: **Plot of UTS Vs % Cr Additions for both As-cast and Age-hardened Conditions.**

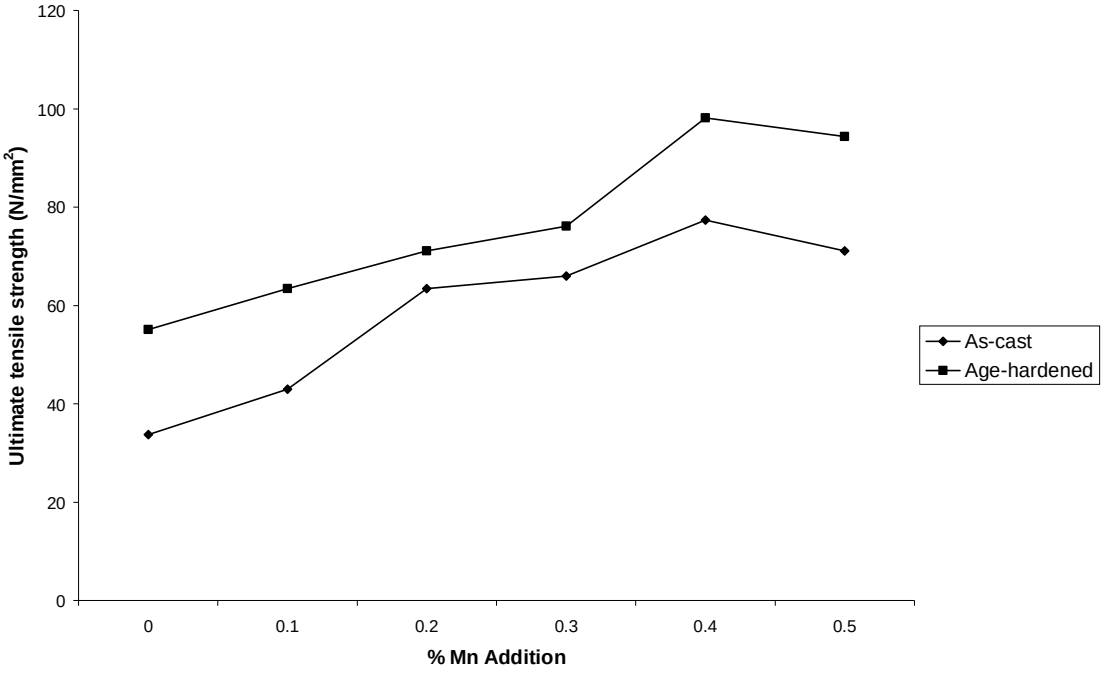


Figure 8: **Plot of UTS Vs % Mn Additions for both As-cast and Age-hardened Conditions.**

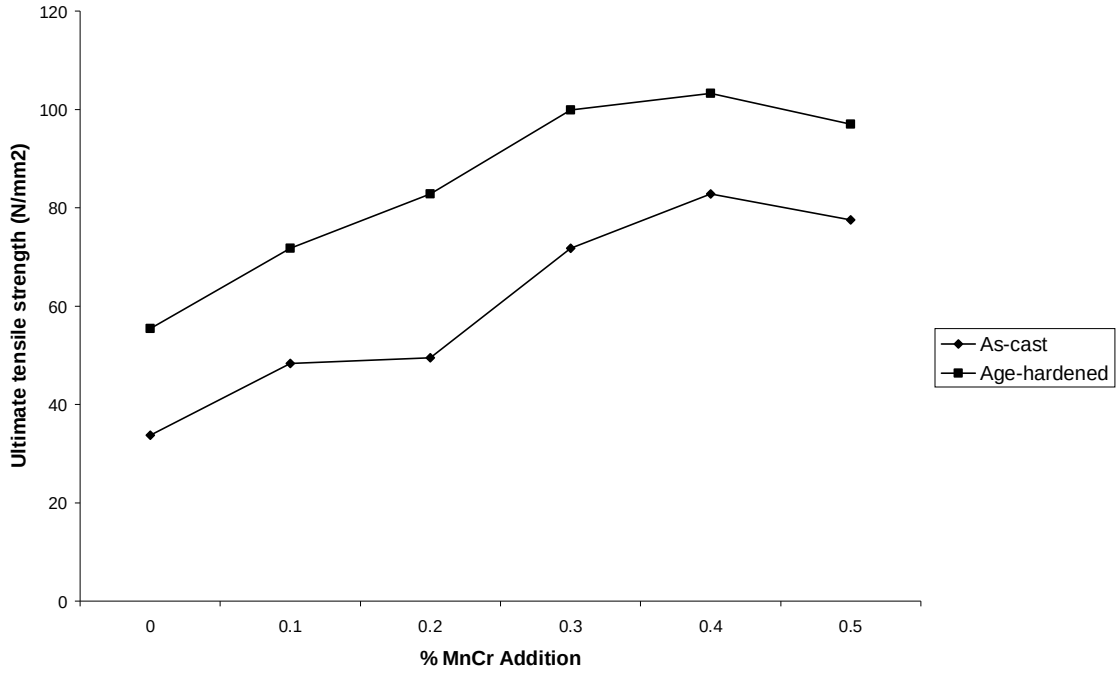
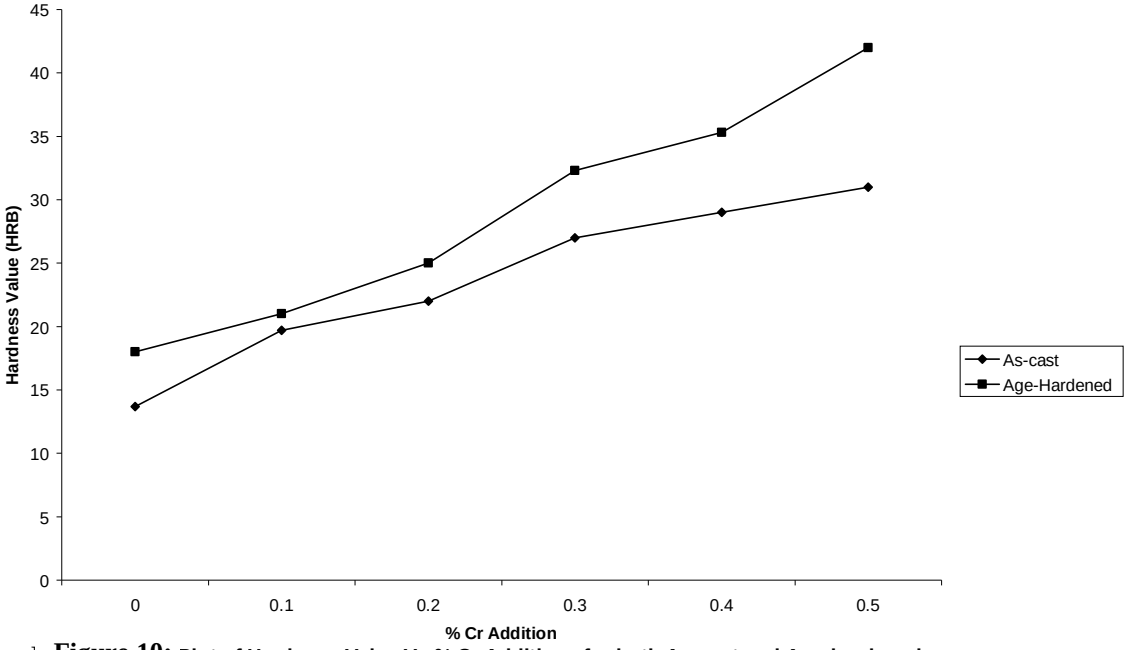


Figure 9: Plot of UTS Vs % MnCr Additions for both As-cast and Age-hardened Conditions.



] **Figure 10: Plot of Hardness Value Vs % Cr Additions for both As-cast and Age-hardened Conditions.**

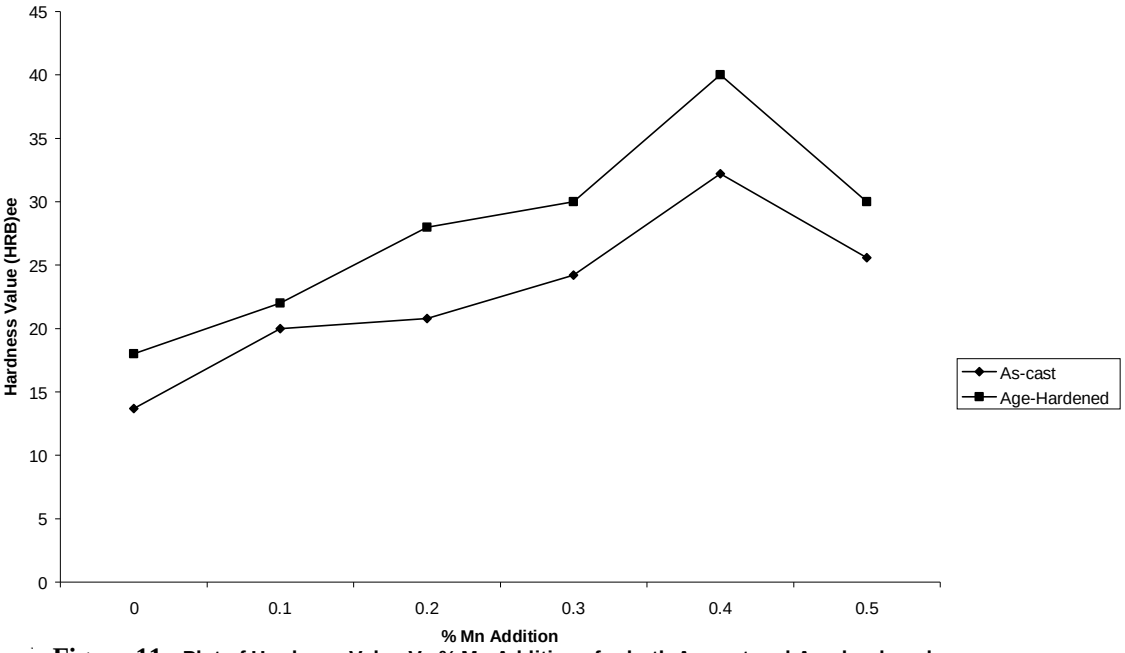


Figure 11: **Plot of Hardness Value Vs % Mn Additions for both As-cast and Age-hardened Conditions.**

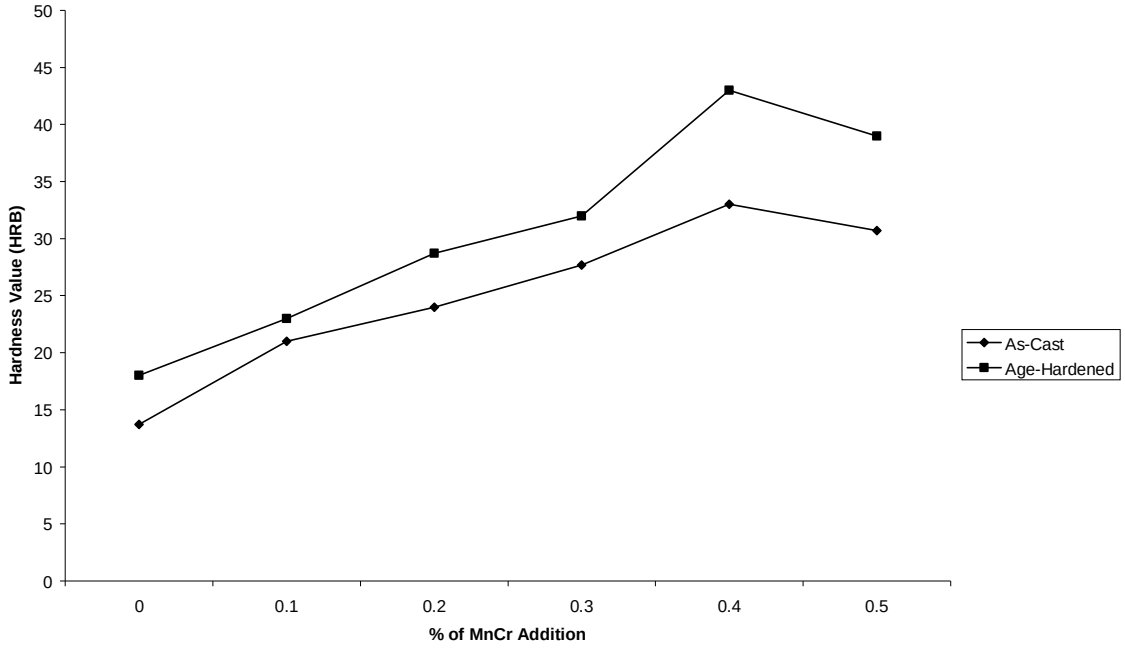


Figure 12: **Plot of Hardness Value Vs % MnCr Additions for both As-cast and Age-hardened Conditions.**

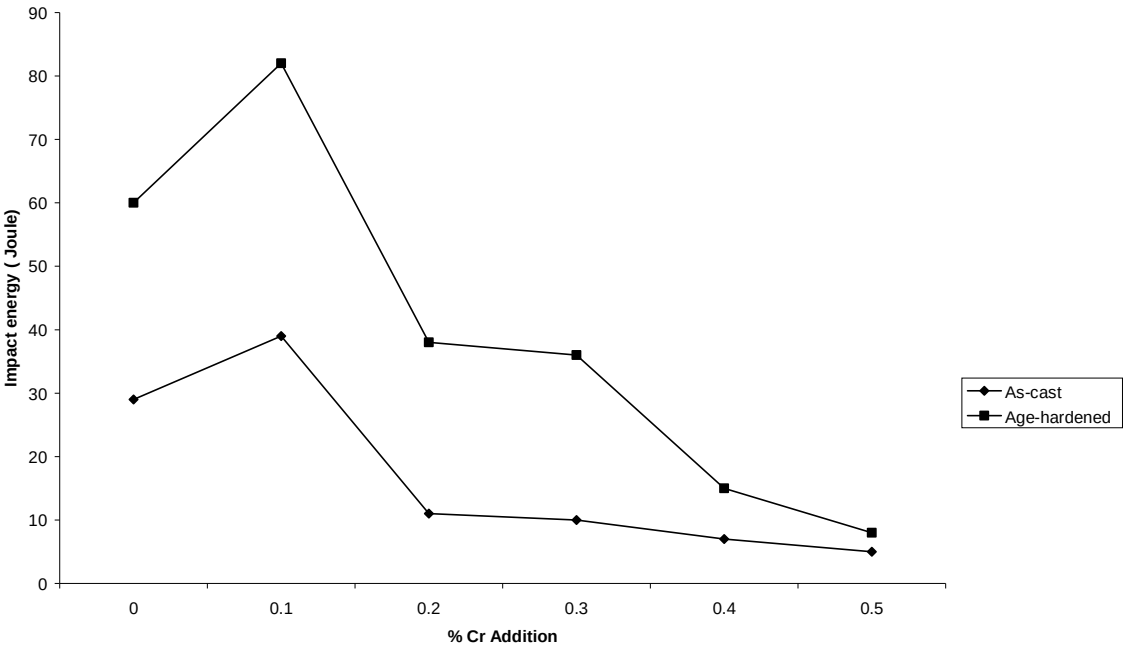


Figure 13: **Plot of Impact Energy Vs % Cr Additions for both As-cast and Age-hardened conditions**

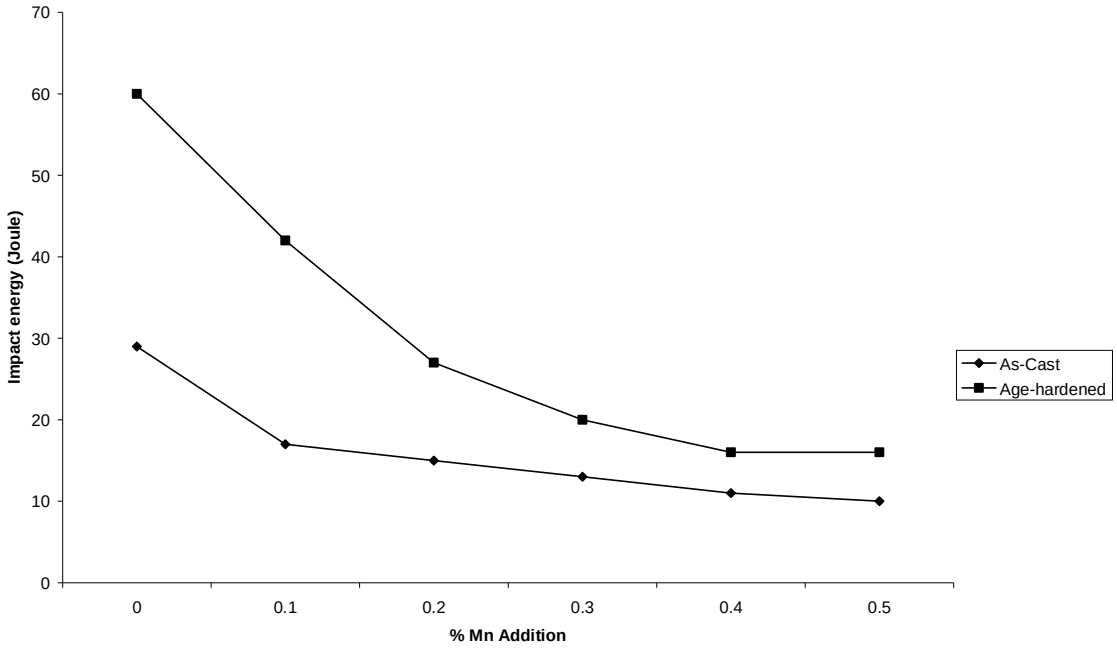


Figure 14: **Plot of Impact Energy Vs % Mn Addition for both As-cast and Age-hardened Conditions**

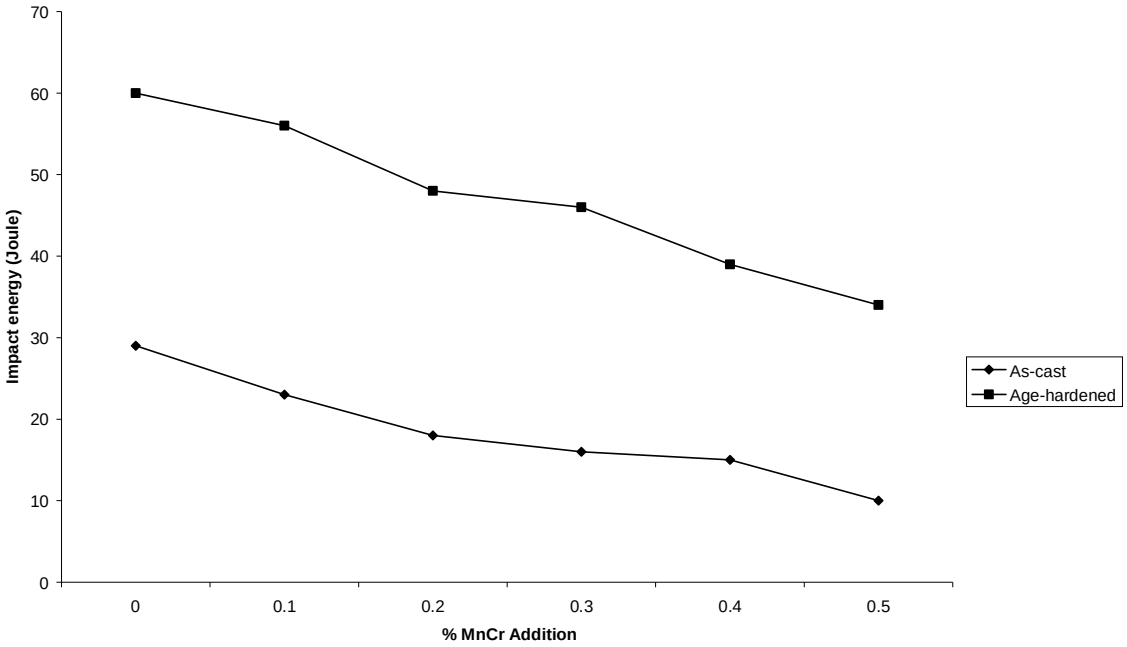


Figure 15: Plot of Impact Energy Vs % MnCr Additions for both As-cast and Age-hardened Conditions

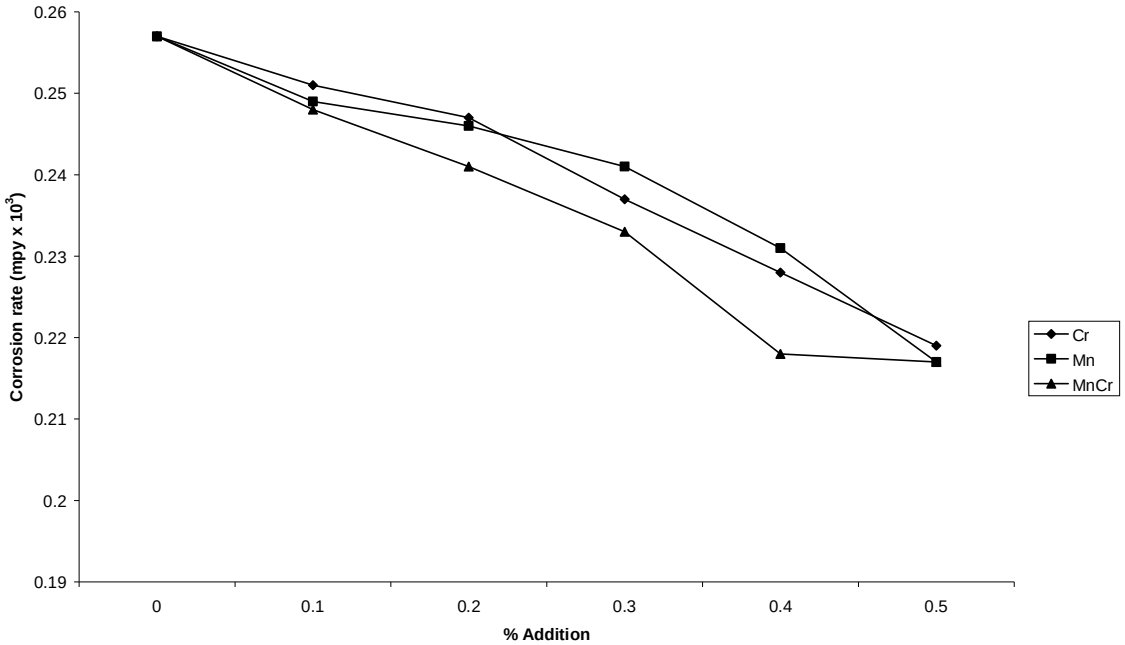


Figure 16: Plot of Corrosion rate Vs % of Additions (Cr, Mn, MnCr) in 0.5M HCl Solution for As-Cast Condition after 20 days of exposure

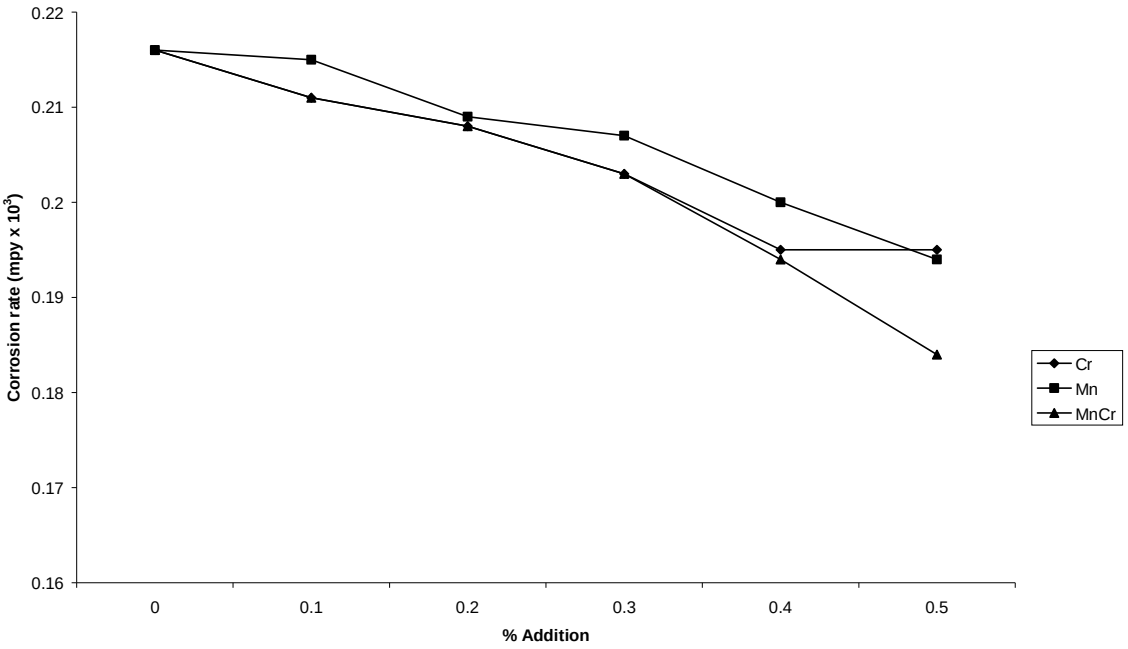


Figure 17: **Corrosion Rate Vs % of Additions (Cr, Mn, MnCr) in o.5M HCl Solution for Age-hardened Condition After 20 days of exposure**

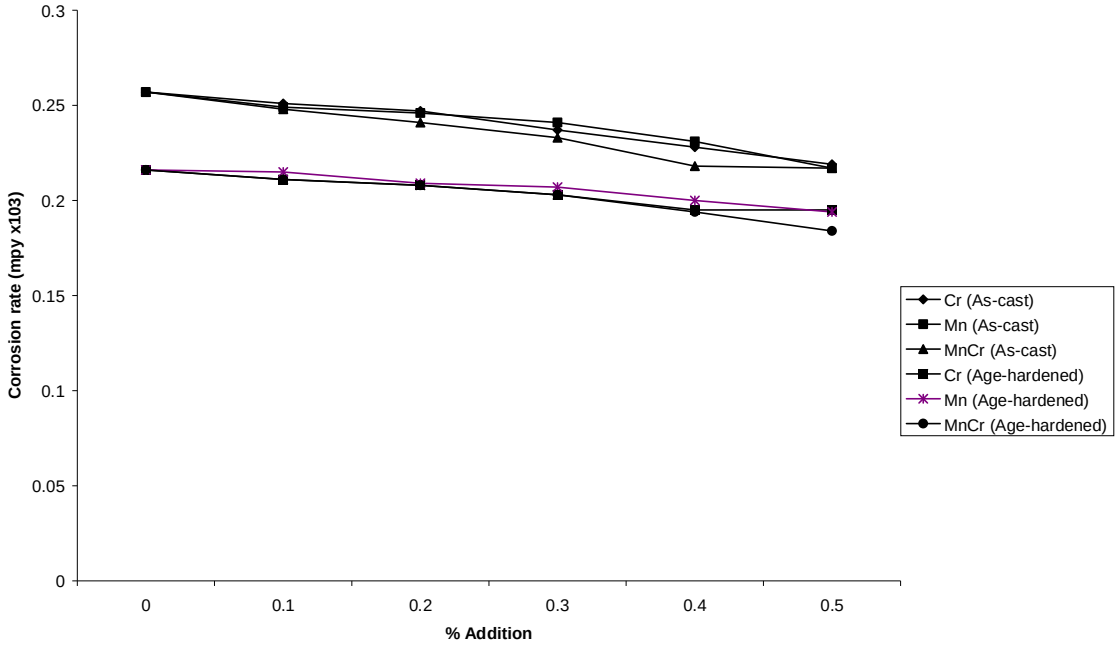


Figure 18: **Corrosion Rate Vs % of Additions (Cr, Mn, MnCr) for As-cast and Age-hardened Condition after 20 days of exposure**

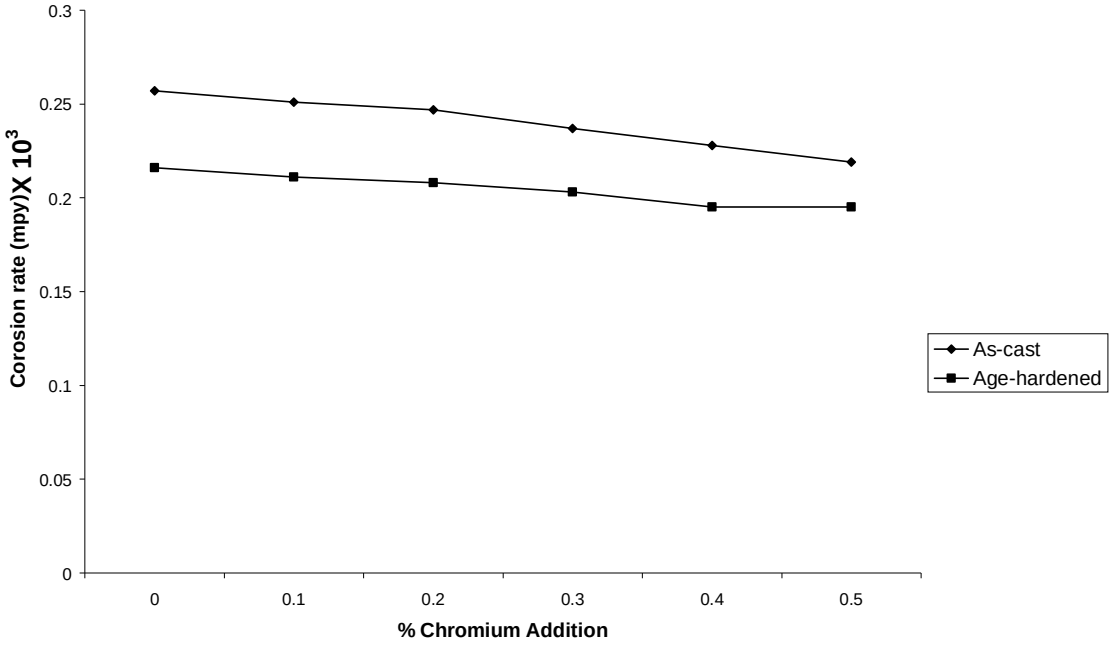


Figure 19: **Corrosion Rate Vs % of Cr Additions in 0.5M HCl solution for both As-cast and Age-hardened Condition for 20 days exposure time**

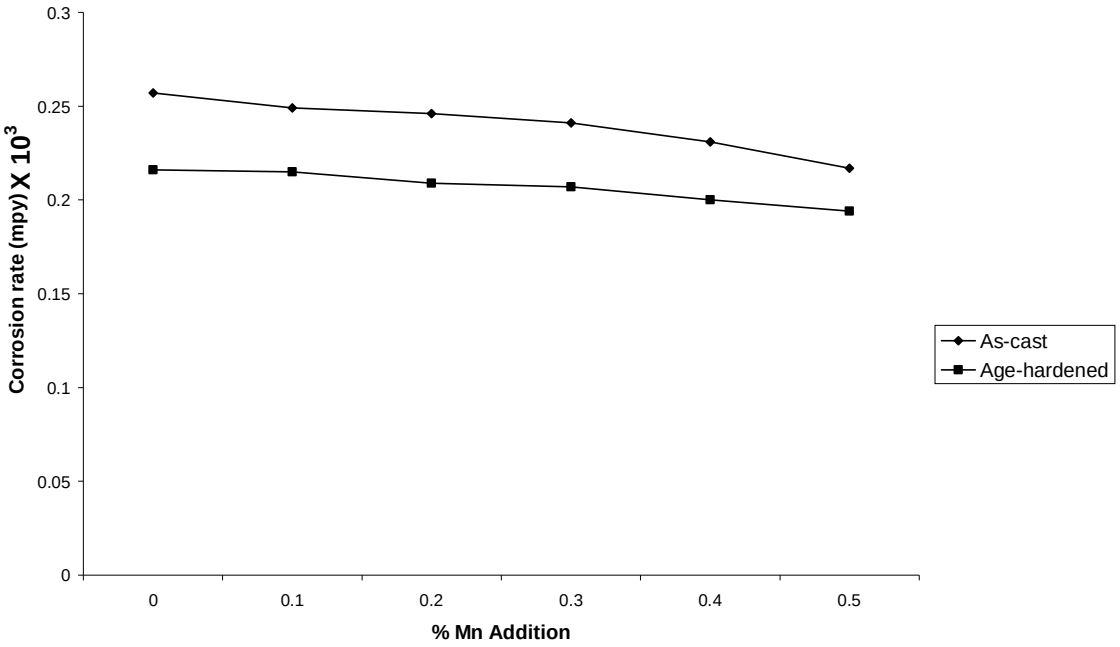


Figure 20: **Corrosion Rate Vs % of Mn Additions in 0.5M HCl solution for both As-cast and Age-hardened Condition for 20 days exposure time**

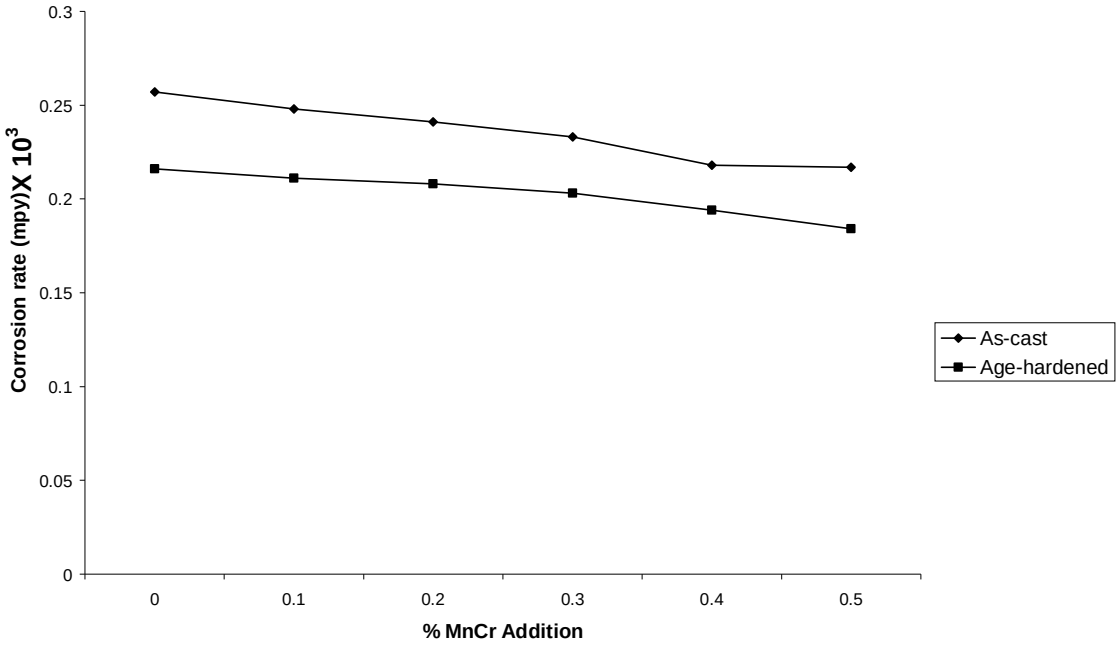


Figure 21: **Corrosion Rate Vs % of MnCr Additions in 0.5M HCl solution for both As-cast and Age-hardened Condition for 20 days exposure time**

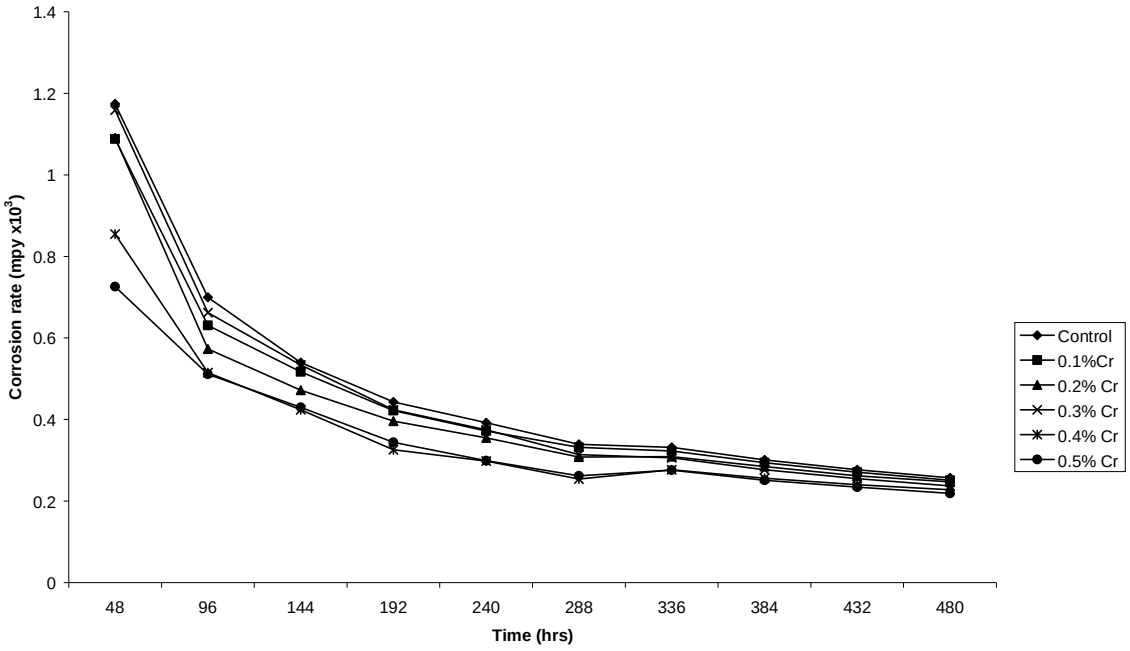


Figure 22: **Corrosion Rate Vs Time of exposure (hrs) for Cr Additions in the As-cast condition**

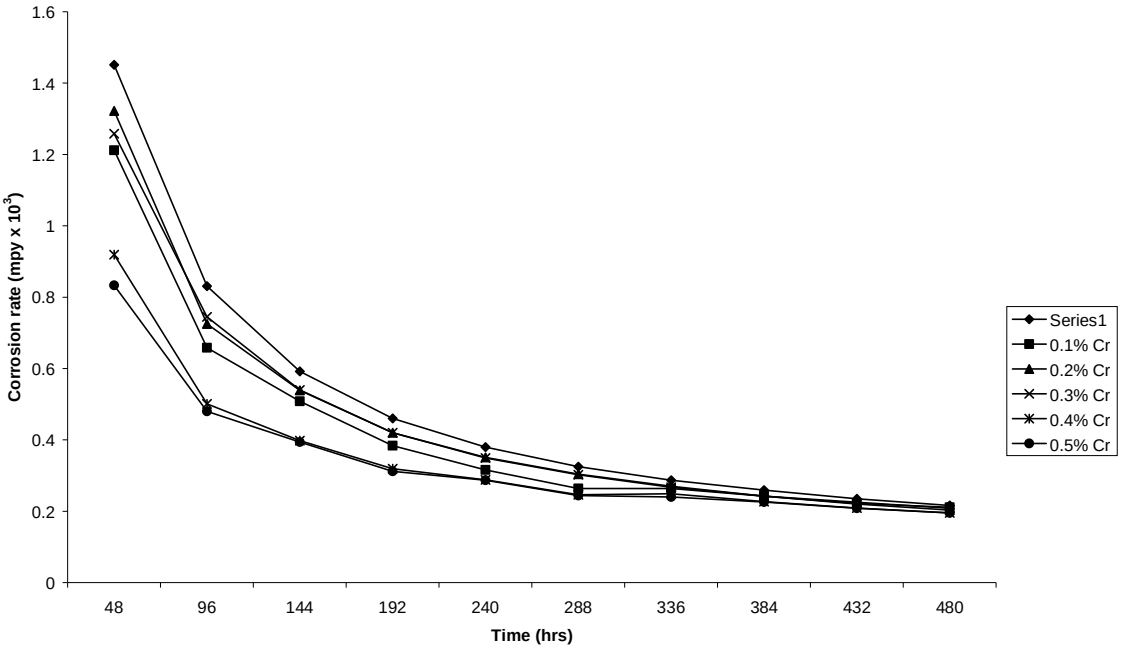


Figure 23: Corrosion Rate Vs Time of Exposure (hrs) for Cr Addition in the Age-hardened condition

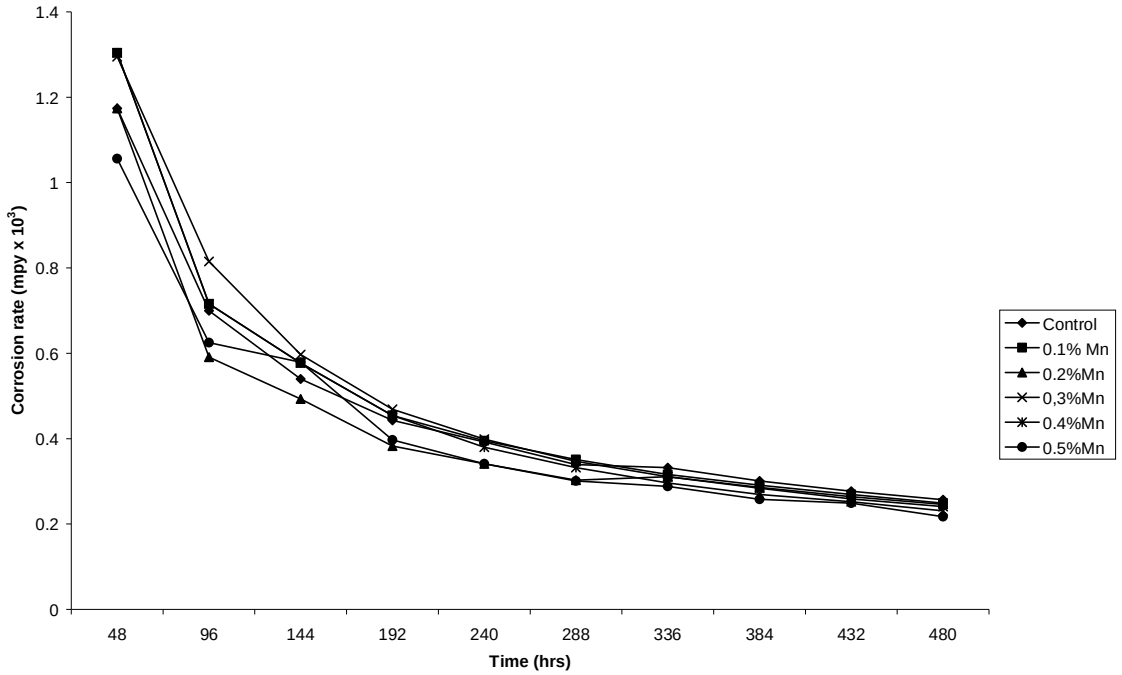


Figure 24: Corrosion Rate Vs Time of Exposure (hrs) for Mn Addition in the As-cast condition

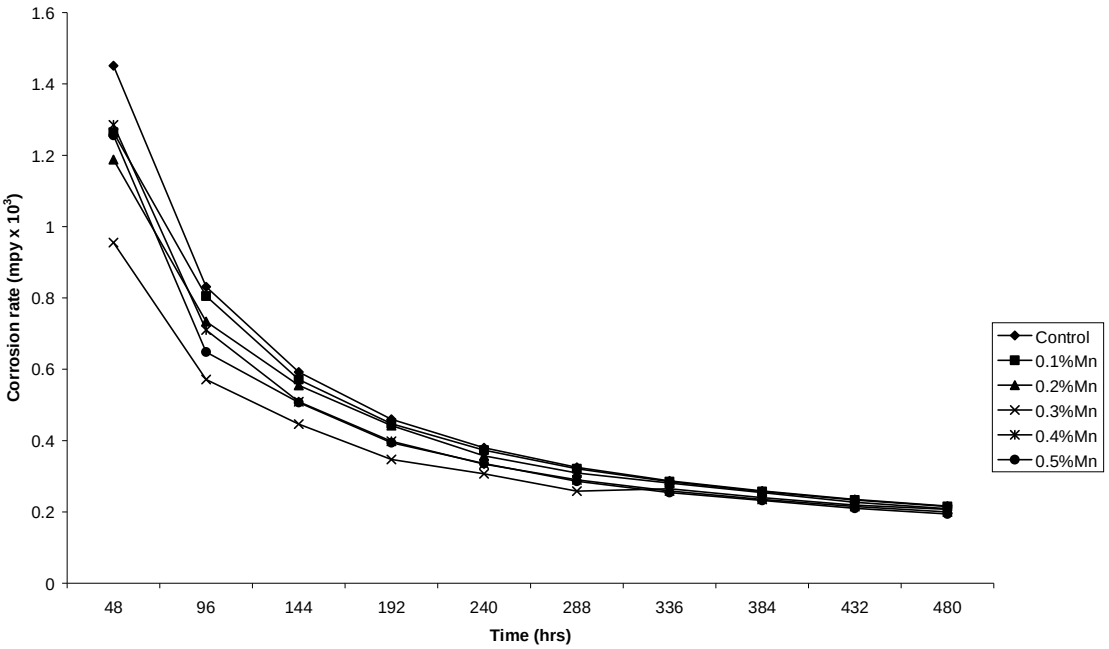


Figure 25: Corrosion Rate Vs Time of Exposure (hrs) for Mn Additions in the Age-hardened condition

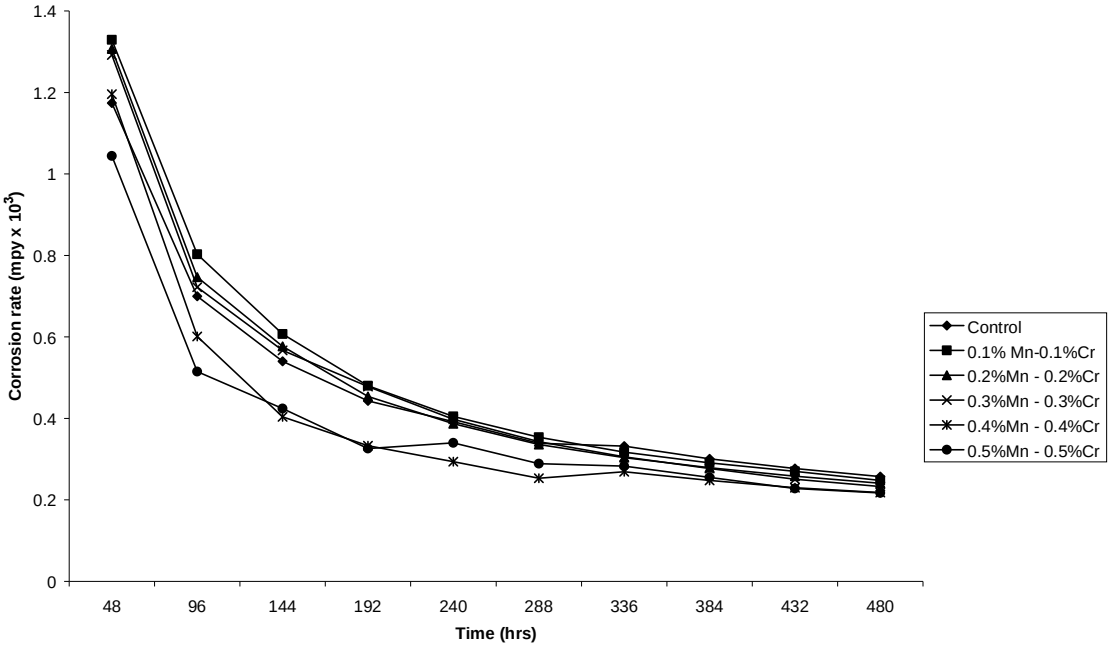


Figure 26: Corrosion Rate Vs Time of Exposure (hrs) for MnCr Additions in the As-cast condition

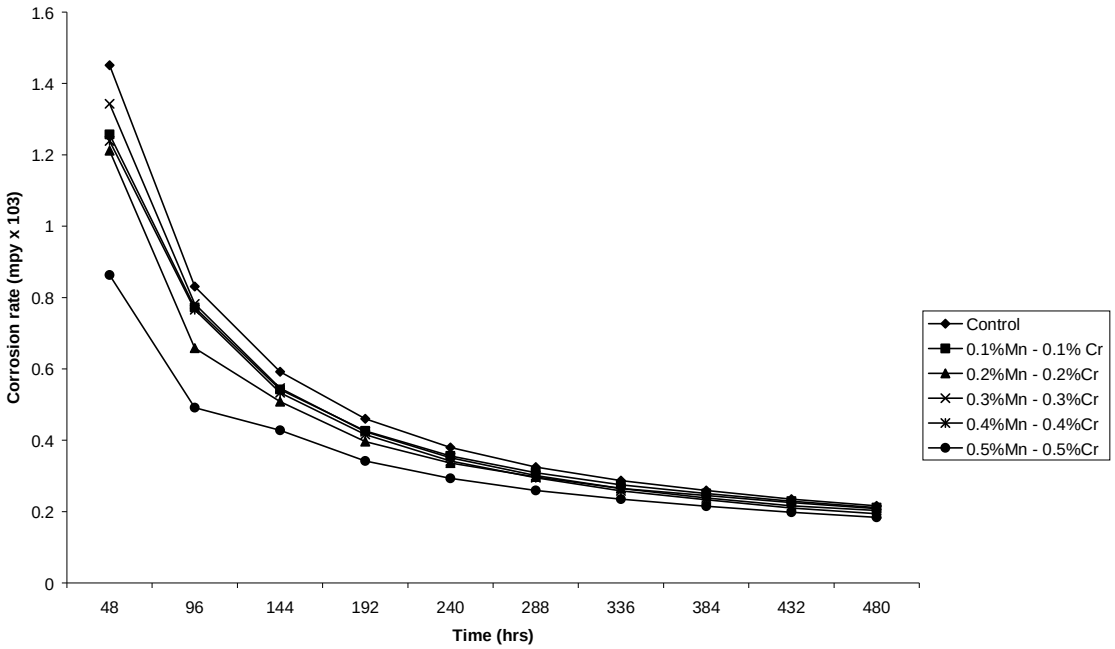


Figure 27: Corrosion Rate Vs Time of Exposure (hrs) for MnCr Additions in the Age-hardened condition